Volume 59
Number 80
14 October 2023
Pages 11885–12040

ChemComm

Chemical Communications

rsc.li/chemcomm

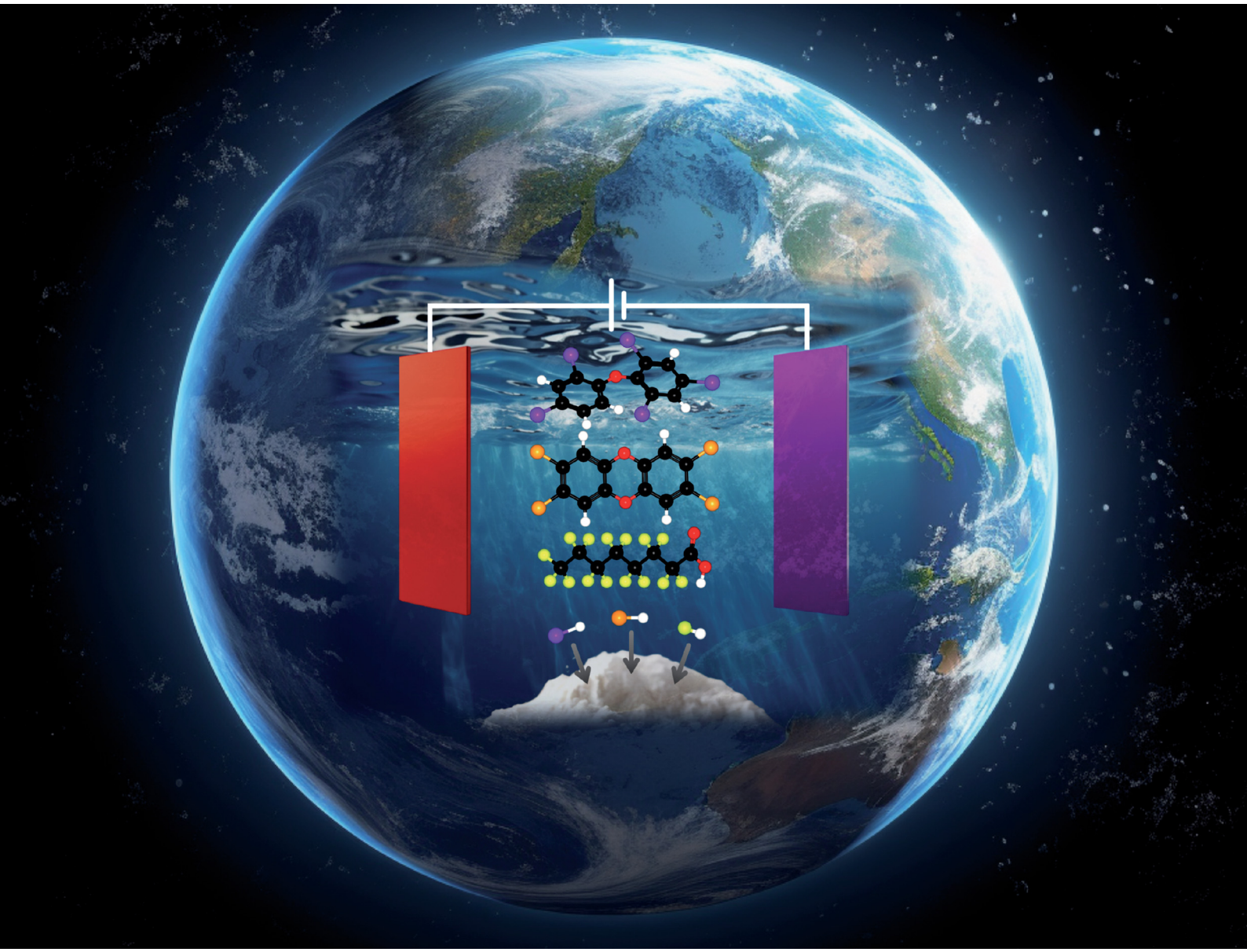

ISSN 1359-7345

ROYAL SOCIETY OF CHEMISTRY

HIGHLIGHT

Astrid M. Müller *et al.*

Advanced electrocatalytic redox processes for environmental remediation of halogenated organic water pollutants

ChemComm

HIGHLIGHT

View Article Online
View Journal | View Issue

Cite this: *Chem. Commun.*, 2023, **59**, 11895

Advanced electrocatalytic redox processes for environmental remediation of halogenated organic water pollutants

Madeleine K. Wilsey,[a] Teona Taseska,[b] Ziyi Meng,[a] Wanqing Yu[b] and Astrid M. Müller *[abc]

Halogenated organic compounds are widespread, and decades of heavy use have resulted in global bioaccumulation and contamination of the environment, including water sources. Here, we introduce the most common halogenated organic water pollutants, their classification by type of halogen (fluorine, chlorine, or bromine), important policies and regulations, main applications, and environmental and human health risks. Remediation techniques are outlined with particular emphasis on carbon–halogen bond strengths. Aqueous advanced redox processes are discussed, highlighting mechanistic details, including electrochemical oxidations and reductions of the water–oxygen system, and thermodynamic potentials, protonation states, and lifetimes of radicals and reactive oxygen species in aqueous electrolytes at different pH conditions. The state of the art of aqueous advanced redox processes for brominated, chlorinated, and fluorinated organic compounds is presented, along with reported mechanisms for aqueous destruction of select PFAS (per- and polyfluoroalkyl substances). Future research directions for aqueous electrocatalytic destruction of organohalogens are identified, emphasizing the crucial need for developing a quantitative mechanistic understanding of degradation pathways, the improvement of analytical detection methods for organohalogens and transient species during advanced redox processes, and the development of new catalysts and processes that are globally scalable.

Received 30th June 2023,
Accepted 11th September 2023

DOI: 10.1039/d3cc03176d

rsc.li/chemcomm

[a] *Materials Science Program, University of Rochester, Rochester, New York 14627, USA. E-mail: astrid.mueller@rochester.edu*
[b] *Department of Chemical Engineering, University of Rochester, Rochester, New York 14627, USA*
[c] *Department of Chemistry, University of Rochester, Rochester, New York 14627, USA*

Madeleine K. Wilsey

Madeleine Wilsey completed her BS degree in chemistry and physics at Western Illinois University in 2019, where she conducted research under the supervision of Prof. Saisudha Mallur and Prof. J. Scott McConnell. After the completion of her undergraduate studies, Madeleine worked as an R&D intern at the company AP Lazer under the supervision of CEO Tong Li. Madeleine joined Prof. Astrid M. Müller's group at the University of Rochester in summer 2020, and she is currently a PhD candidate investigating sustainable electrocatalysis for selective conversions of hydrocarbons into alcohols, using bimetallic nanocatalysts made by pulsed laser in liquids synthesis.

Teona Taseska

Teona Taseska, native of Ohrid, North Macedonia, came to the U.S. for her undergraduate education at the University of Rochester, where she is a rising senior in chemical engineering, clustering in Japanese. She has won the 2021 MLC Book Award for Japanese Language. She has been conducting undergraduate research in the lab of Prof. Astrid M. Müller since her sophomore year. Her research projects focus on opportunities for climate-friendly catalysis technologies to meet human needs on a global scale, hydrogen peroxide electrosynthesis, and the development of processes for the destruction of PFAS chemicals in aqueous systems, electrocatalyzed by laser-made nanomaterials.

Introduction

The industrial revolution led to unprecedented technological progress, human health, prosperity, wellbeing, and population growth, but it also caused climate change[1] and environmental pollution on a global scale. Technological innovations in consumer goods, and pharmaceutical, agricultural, and industrial applications released large quantities of halogenated organic pollutants into the environment, including Earth's waterways. Electrocatalytic technologies that remediate halogenated organic water pollutants can learn from other electrocatalysis fields and adapt analogue concepts, for example from water oxidation[2–5] and oxygen reduction electrocatalysis,[2,6–8] aqueous photoelectrochemical mechanisms,[9–12] *in situ* and *operando* spectroscopies of electrocatalysts,[13–15] and computational electrocatalyst design.[15–17]

Halogenated organic water pollutants are hazardous for humans and animals.[18–27] They are organic compounds that contain the halogen atoms fluorine, chlorine, or bromine, possess solubility in natural water, and are harmful to the environment. Halogenated organic compounds, also called organohalogens, are typically classified into different categories depending on their structure or chemical properties. Halogenated organic water pollutants include aliphatic or aromatic halogenated hydrocarbons.[28] Common organohalogens are shown in Fig. 1. Organohalogens serve as solvents, coatings, degreasing agents, biocides, medical propellants, plasticizers, hydraulic and heat transfer fluids, chemical synthesis intermediates, refrigerants, coolants, and flame retardants.[22,23,25,27] Organohalogens possess exceptionally strong carbon–halogen bonds, leading to high heat resistance, low surface tension, high lipophilicity, and chemical inertness. Most organohalogens possess amphiphilic (ionic and neutral) properties and are xenobiotic, although natural organohalogens are known.[29] Because of their thermodynamically strong covalent C–X (X = F, Cl, or Br) bonds, these compounds were initially considered nonmetabolizable and nontoxic,[30] which turned out to be false, creating global human health risks and an urgent need for environmental remediation, particularly from water sources.

The discovery and manufacturing of organohalogens has led to revolutionary materials with high utility, such as non-stick Teflon cookware coatings, Rain-X water repellants, fire-retardant, water-proofing, and grease-resisting additives to upholstery and clothing, firefighting foams, and cleaning agents for electronics and microelectronics manufacturing. The widespread use of these chemicals has resulted in inadvertent or purposeful discharge into the environment.[31] The high strength of carbon–halogen bonds inhibits biodegradation processes in nature, and leads to extended lifetimes and

Ziyi Meng

Ziyi Meng obtained his BSc in Polymer Materials and Engineering (2019) and MSc in Materials Science (2022) at Hubei University of Technology (China), where he conducted research in microbial modified mineral materials, advanced functional super elastic, and inorganic–organic composited proton exchange membrane fuel cells for extreme conditions under the supervision of Prof. Qingting Liu. In 2022, he enrolled at the University of Rochester as a PhD student in the Materials Science Program and joined the group of Prof. Astrid M. Müller to work on the degradation of per- and polyfluoroalkyl substances (PFAS), employing aqueous electrocatalysis and laser-made bimetallic nanomaterials.

Wanqing Yu

Wanqing Yu hails from Guangzhou, China, and came to the U.S. for her undergraduate education at the University of Rochester, where she obtained dual-major BS and BA degrees in chemical engineering and dance in 2023. At the University of Rochester, she conducted undergraduate research in the group of Prof. Astrid M. Müller, working on aqueous electrocatalytic defluorination of the PFAS chemical perfluorooctanoic acid, catalyzed by nanomaterials made by pulsed laser in liquids synthesis. In fall 2022, Wanqing received an Undergraduate Teaching Assistant Award in chemical engineering. Currently, Wanqing is a PhD student in chemical engineering at Georgia Institute of Technology.

Astrid M. Müller

Astrid M. Müller is an Assistant Professor of Chemical Engineering at the University of Rochester since 2018. Prof. Müller earned a PhD in Physical Chemistry for work on ultrafast reaction dynamics at the Max Planck Institute of Quantum Optics. Her postdoctoral work centred on developing a fundamental understanding of laser–matter interactions. Her independent research focuses on pulsed laser in liquids synthesis of mixed-metal nanomaterials with controlled structural and electronic properties. This uniquely positions Prof. Müller's group to quantitatively understand how nanocatalysts and electrocatalytic mechanisms impact the performance of nanomaterials in sustainable energy, green chemistry, and aqueous PFAS destruction applications.

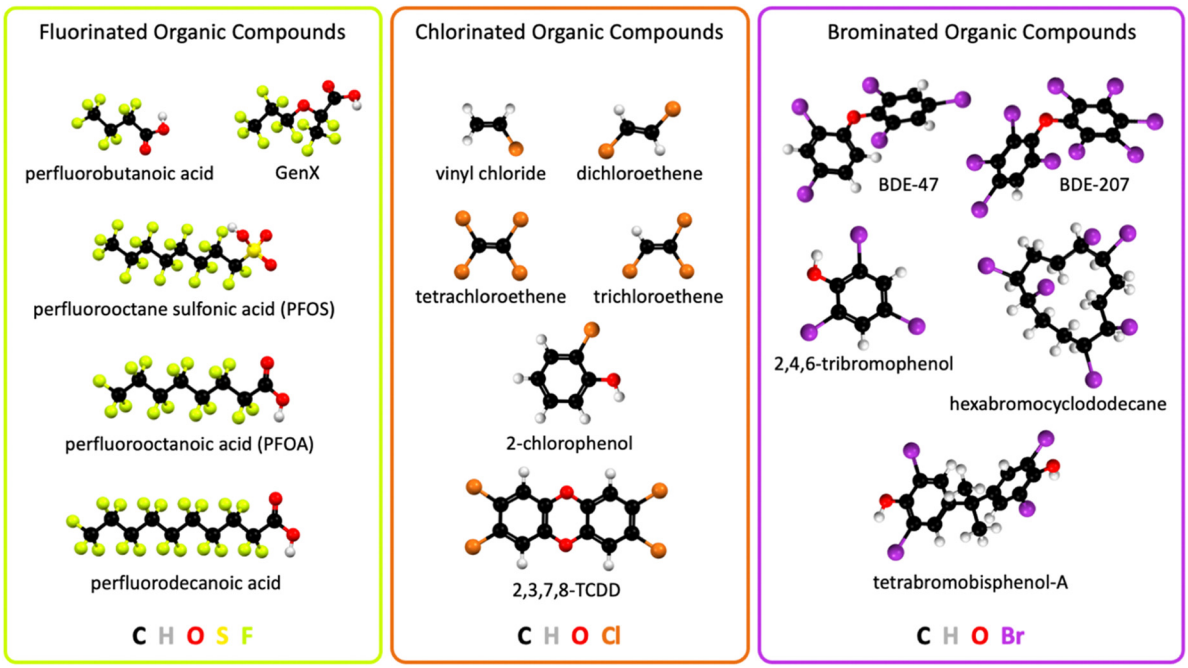

Fig. 1 Chemical structures of widespread halogenated organic water pollutants; 2,3,7,8-TCDD, 2,3,7,8-tetrachlorodibenzodioxin; BDE, bromodiphenyl ether.

accumulation of chlorinated, brominated, and fluorinated organic compounds in the environment, animals and humans.[20]

Policy regulations and restrictions regarding the manufacturing and use of halogenated organics have been instated on the national level and worldwide. For example, restrictions on the production of polychlorinated biphenyls (PCBs) began in 1970s, followed by international implementations through the Stockholm Convention in 2004, which banned the production of PCBs, aiming to phase out PCBs in use by 2025, and ensuring environmentally sound management by 2028.[32] Limitations on brominated compounds started in 2009 when the Stockholm Convention listed polybrominated diphenyl ethers as new persistent organic pollutants and banned their production and use.[33] Currently, five specific groups of brominated flame retardants are listed in the Stockholm Convention: hexabromobiphenyl, hexabromocyclododecane (HBCD), and the commercial polybrominated diphenyl ethers octabromodiphenyl ether (octaBDE), pentabromodiphenyl ether (pentaBDE), and decabromodiphenyl ether (decaBDE).[33]

Additional policy efforts have been made to discontinue or limit the production and use of poly-fluorinated compounds. Significant New Use Rules were established in the U.S. to restrict the production and use of per- and polyfluoroalkyl substances (PFAS). The U.S. Environmental Protection Agency worked with leading chemical companies on a global phaseout of perfluorooctanoic acid (PFOA) through the 2010/2015 PFOA Stewardship Program to reduce emissions and residual content of PFAS.[34] By 2009, perfluorooctane sulfonic acid (PFOS) and related compounds were listed under Annex B of the Stockholm Convention on Persistent Organic Pollutants.[35] The U.S. Environmental Protection Agency's notification levels for PFOA and PFOS are 5.1 and 6.5 ppt, respectively, and the response levels for PFOA and PFOS are 10 and 40 ppt, respectively.[36,37]

Chlorofluorocarbons (CFCs) and hydrochlorofluorocarbons (HCFCs) are fully or partially halogenated hydrocarbons that are produced from methane, ethane, and propane. CFCs and HCFCs are nontoxic, non-flammable, and long-lived synthetic compounds that contain carbon, hydrogen, chlorine, and fluorine.[38] Any production of CFCs was banned in 2010 through the Montreal Protocol to reduce CFC emissions into the atmosphere, where CFCs deplete stratospheric ozone.[39]

Applications and health risks of halogenated organic water pollutants

Exposure to organohalogens threatens human health.[40–42] Resistance to biodegradation causes long lifetimes and accumulation of organohalogens in the environment, together with global distribution *via* waterways.[43] Bioaccumulation through food chains and direct uptake introduce organohalogens into the human body, where they have been linked to Parkinson's disease,[44] harm in cognitive function and development, reproductive, hormonal, and metabolic processes, and increased risk for cancer.[30,45,46] Specific applications and associated risks of chlorinated, brominated, and fluorinated organic compounds are detailed below.

Chlorinated and brominated organic water pollutants. Chlorinated and brominated organic water pollutants are harmful to human health and the environment.[46,47] They accumulate in living organisms.[46] Chlorinated organic compounds found uses in metal working fluids, lubricants, flame retardants, and plasticizers.[48] Polybrominated diphenyl ethers

(PBDEs), polybrominated biphenyls (PBBs), tetrabromobisphenol-A (TBBPA), polybrominated phenols (PBPs), polychlorinated biphenyls (PCBs), polychlorinated dibenzo-*p*-dioxins and dibenzofurans (PCDD/Fs), polybrominated dibenzo-*p*-dioxins and dibenzofurans (PBDD/Fs), and chlorinated polycyclic aromatic hydrocarbons (ClPAHs) are used in the manufacturing of electronic equipment and devices and remain in electronic waste (e-waste), creating serious pollution challenges in e-waste recycling.[49]

The high stability and environmental persistence of chlorinated organic compounds is attributable to the lipophilicity and high thermodynamic strength of C–Cl bonds.[50,51] Common chlorinated organic water pollutants are polychlorinated dibenzodioxins (PCDDs), polychlorinated dibenzofurans (PCDFs), PCBs, and chlorinated paraffins, whose global annual production exceeded 1 million metric tons in 2009,[22] the year chlorinated compounds started to get restricted. Chlorinated alkanes are toxic: human exposure can harm the liver, kidneys, lungs, neurological systems, cardiovascular system, and immune system, and they have been linked to increased risk of cancer (Fig. 2).[52] Although the production of PCBs has been phased out decades ago, 10 million tons of PCB-containing materials remain across the globe.[32] PCBs accumulate in fat, liver, skin, and nerve tissues in humans (Fig. 2).[20] Compounds produced by PCB detoxification in the liver have been linked to hormonal interference, reproductive,[53,54] metabolic,[55] and neurological dysfunction,[56] and cancer (Fig. 2).[57] The extent of toxicity depends on the chemical structure of chlorinated organic compounds and particularly the position of chlorine atoms on phenyl rings, with the highest toxicity observed for chlorine in *meta* and *para* positions.[58] Dioxins have been linked to similar reproductive, neurological, and carcinogenic issues as PCBs.[20] Chlorinated organic compounds often originate in small organisms and transfer through food chains to accumulate in higher-order species in large doses.[20]

Most brominated organic water pollutants are commonly known as brominated flame retardants (BFRs), which are used across many industries to inhibit or suppress combustion processes. BFRs are often found in plastics, textiles, electronic circuitry, and building materials.[49,59] The utility of BFRs has led to a growing market with a global market size of 2.14 billion USD in 2022 and a compound annual growth rate of 5.7%.[60] BFRs are lipophilic and bioaccumulate if leached from products, during manufacturing, or during incineration.[61] Brominated, like chlorinated, organic pollutants accumulate in the environment and threaten human health by build-up in lipid tissues.[20] Specific health effects caused by BFRs are less understood than those of PCBs. BFRs have been linked to interfering with nerve development in fetuses and newborns, and harming infant cognitive function (Fig. 2).[20,62]

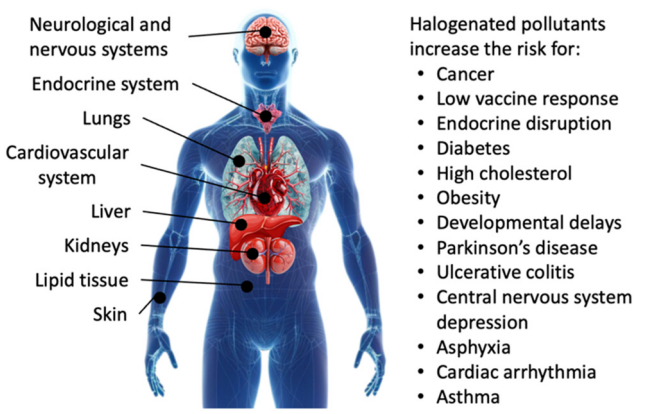

Fig. 2 Human health risks upon exposure to halogenated organic water pollutants.

Fluorinated organic water pollutants. Organofluorine compounds have widely been used in industry because of high heat resistance, low surface friction, and chemical inertness.[63] The exceptional utility, concomitant broad use, and chemical resistance of materials that contain C–F motifs, together with detrimental human health effects have led to concerns about accumulation of fluorinated chemicals; specific health and environmental effects are detailed below, organized by class of fluorinated organic pollutants.

Partially fluorinated solvents. Partially fluorinated solvents are commonly utilized in pharmaceuticals, as surfactants, and in energy devices.[64–66] Partially fluorinated solvents are pollutants because they contribute to ozone depletion, global warming, bioaccumulation, and toxicity, especially in drinking water supplies,[67] leading to elevated risk of thyroid disease, high cholesterol, ulcerative colitis, kidney cancer, testicular cancer, and pregnancy-induced hypertension (Fig. 2).[68]

Chlorofluorocarbons and hydrochlorofluorocarbons. The most widely known representatives of CFCs and HCFCs are Freons. Trichloro(fluoro)methane (also known as Freon-11, CFC-11, or R-11) and dichlorodi(fluoro)methane (also known as Freon-12, CFC-12, or R-12) are primarily used as coolants in air conditioning and refrigeration applications, blowing agents in foams, insulation, packing materials, propellants in aerosol cans, and solvents.[69] Chloro(trifluoro)methane (also known as Freon-13, CFC-13, or R-13) is predominantly employed in the manufacturing of semiconductor chips, in vapor degreasing, and in cold immersion cleaning of microelectronic components, or as a solvent in procedures for surface cleaning in the electronics industry.[69] Chloro(difluoro)methane (HCFC-22), 1-chloro-1,1-difluoroethane (HCFC-142b), and 1,1-dichloro-1-fluoroethane (HCFC-141b) are mainly used as refrigerants and blowing agents in foams.[70] CFCs are acutely toxic upon inhalation; adverse effects include central nervous system depression, asphyxia, and cardiac arrhythmia (Fig. 2).[71] HCFCs are more flammable and more susceptible to decomposition during use than CFCs, by which toxic byproducts can be formed.[72,73] Hydrofluorocarbons (HFCs) gradually replace CFCs and HCFCs because they are generally less toxic than HCFCs for aquatic life, terrestrial plants, and mammals, including humans.[73] The flammability of HFCs is higher than that of CFCs and HCFCs.[74] HFCs possess very low solubility in water, making them insignificant water pollutants.[73]

Per- and polyfluorinated substances (PFAS). PFAS are heat-, water-, and oil-resistant synthetic chemicals that are widely

used in consumer, commercial, and industrial products,[75] from aerospace to food production.[76] Fluoropolymer coatings can repel water and oil, and resist thermal, chemical and biological decomposition. Decades of heavy use have resulted in bioaccumulation and contamination of water, soil, animals, and people all over the world.[77] PFAS accumulation has even been observed in Antarctica.[78] For example, PFOA has a half life of 3.8 years in humans, and PFOS accumulates in the human liver and is trapped by bile acid transporters, resulting in a half life of 7.1 years in humans.[79] PFAS exposure is harmful to human health.[80,81] The extreme chemical stability of PFAS arises from numerous C–F bonds, which is beneficial for the durability of products, but problematic for the environment and ultimately human health, as PFAS resist biodegradation.

PFAS have been identified in ground water, surface water, drinking water, soil, indoor air, dietary sources, manufacturing locations, and wastewater treatment plants, as well as in human blood, serum, milk, urine, and placenta tissue.[82] For example, the PFAS chemical PFOS bioaccumulates in fish that humans consume, making such fish a source of human PFAS exposure.[83] Human PFAS exposure can additionally occur *via* dermal contact because PFAS can be taken up from oil- and water-resistant non-stick coatings on cookware and paper food packaging materials.[83] Inhalation of indoor air and household dust is another route for human PFAS uptake.[83]

Human exposure to PFAS causes reproductive and immune system harm, increased risk of non-Hodgkin's lymphoma and kidney, testicular, prostate, breast, liver, and ovarian cancers, decreased vaccine response, increased risk of asthma in adolescents, increased risk of diabetes and hypertension in women, developmental delays in children, changes in liver enzymes, endocrine disruption, and increased cholesterol levels and/or risk of obesity;[80,81,84–89] in unborn children, delayed mammary gland development, reduced response to vaccines, and lower birth weight have been observed (Fig. 2).[90,91] PFAS also pose ecological risks through bioaccumulation, food chains, and toxicity in terrestrial and aquatic wildlife.[92]

Remediation techniques for halogenated organic water pollutants

Maximum contaminant limits in water in the U.S. are set by the U.S. Environmental Protection Agency and published in the National Primary Drinking Water Regulations.[93] For most chlorinated, brominated, and fluorinated organic pollutants, the allowable contamination threshold is on the order of parts per billion (ppb) or parts per trillion (ppt), depending on the compound and associated risks.[52,94] To achieve safe levels, water remediation techniques are needed for effective removal and destruction of pollutants. Halogenated organic pollutants have a particularly high resistance against degradation because of their strong carbon–halogen bonds. As a result, only a few destruction techniques for complete mineralization of halogenated organic water pollutants have been commercialized, and the field is a very active research area.[27,95,96] Several separation techniques have found commercial use to remove halogenated pollutants from water sources; separation only concentrates pollutants,[27] after which disposal by destruction is necessary.

Concentration *vs.* destruction techniques

Organohalogen concentrations differ vastly across water sources and mainly depend on the distance from the location of pollutant discharge. For example, PFAS concentrations in water range from 26 to 5200 ng L^{-1};[97,98] for illustration, the lower limit corresponds to approximately one drop in an Olympic swimming pool full of water. Freshwater sources are typically contaminated with PFAS at levels on the order of hundreds of nanograms per liter, whereas concentrations in marine water are at tens of nanograms per liter.[98]

Concentration techniques. Halogenated organic compounds have been separated from water by nitrifying fluidized-bed biomass[99] or by distillation, taking advantage of volatility differences between organohalogens and water before discharging the water into sewage systems.[100] Adsorption and reverse osmosis separation methods have been described to concentrate chlorinated and brominated organic pollutants from dilute natural water sources.

Adsorption techniques. Adsorption utilizes physical or chemical interactions between the surface of a solid (adsorbent) and a solute (adsorbate) to remove pollutants from water sources. In contrast, absorbents are porous materials that take up matter into spaces within and throughout the material. Adsorbable organic halogens are removed from water by adsorption methods,[101,102] such as Pd/Fe bimetallic particles to treat activated sludge of chemical dyestuff wastewater.[103] Granular activated carbon and powdered activated carbon are the most frequently used adsorbents, but activated alumina and zeolites have also been employed.[104] Two common chlorinated groundwater pollutants, tetrachloroethylene and trichloroethylene, have shown significant adsorption on granular activated carbon.[105] Likewise, absorbent materials that are capable of removing brominated water pollutants include metal organic frameworks,[106] biochar,[107] and microplastics.[108]

Reverse osmosis. Reverse osmosis is a separation technique that passes water through a semi-permeable membrane that discharges a treated stream (permeate) and a rejection stream (concentrate). Reverse osmosis decreased the concentration of 2,3,7,8-substituted polychlorinated dibenzo-*p*-dioxins (PCDD), dibenzofurans (PCDFs), and dioxin-like PCBs in water.[109]

Destruction techniques. Destruction of organohalogens is preferable over standalone separation. Separation pre-treatment procedures are often used to increase organohalogen concentrations in water to enhance degradation efficiency[110–112] by overcoming substrate mass transport limitations that are inherent with dilute solutions. Destruction techniques cleave carbon–halogen bonds to produce carbon chemicals that are less harmful than organohalogens, ultimately CO_2, and halogen-containing non-water-soluble mineral-like solids, which is called mineralization.[113–115] Reported destruction methods for pollutant

Table 1 Bond dissociation energies for different binding motifs of halogens X for common organohalogens. Energy ranges originate from different bond dissociation energies depending on the position of the F atom within the molecule. PFOA, perfluorooctanoic acid; PFOS, perfluorooctane sulfonic acid. From ref. 116–123

X	R–X	Bond dissociation energy (kJ mol^{-1})
F	GenX–F	536.0
	HF_2C–F	534.7
	H_5C_6–F	526.0
	H_2FC–F	499.2
	$HO_2C_8F_{14}$–F (PFOA)	451.9–494.1
	H_3C–F	452.3
	$O_3SC_8F_{16}$–F (PFOS)	415.6–461.9
Cl	H_5C_6–Cl	400.0
	$(H_3C)_3C$–Cl	359.4
	$H_3CH_2CH_2C$–Cl	356.9
	H_3CH_2C–Cl	354.4
	H_3C–Cl	334.7
	H_2ClC–Cl	328.4
	HCl_2C–Cl	316.3
	$H_5C_6H_2C$–Cl	302.1
Br	H_5C_6–Br	337.0
	$(H_3C)_3C$–Br	304.2
	$H_3C(H_2C)_2$–Br	303.3
	H_3CH_2C–Br	302.9
	H_3C–Br	291.1
	H_2BrC–Br	280.3
	HBr_2C–Br	266.9
	$H_5C_6H_2C$–Br	248.5

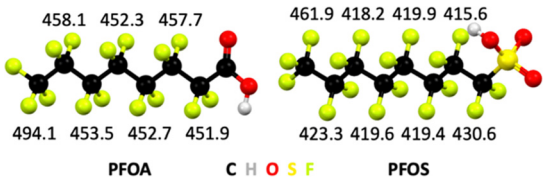

Fig. 3 Bond dissociation energies in kJ mol^{-1} of C–F bonds by position in perfluorooctanoic acid (PFOA) and perfluorooctane sulfonic acid (PFOS). From ref. 122 and 123.

remediation include electrochemical, photochemical, mechanochemical, thermochemical, and advanced oxidation processes, or combinations of these approaches.[27] The exceptionally high thermodynamic stability of carbon–halogen bonds in organohalogens poses the most significant challenge for destruction efficiency; C–X (X = F, Cl, or Br) bond dissociation energies of common organohalogens are in Table 1.

The bond dissociation energy values, which are a measure for thermodynamic bond strength, show that halogen atoms with higher electronegativity form stronger bonds to carbon atoms (Table 1). Fluorine is the most electronegative element in the periodic table and ergo C–F bonds are the strongest covalent bonds known in organic chemistry. In general, electronegativity of halogens follows F > Cl > Br, and likewise the trend in bond strengths follows C–F > C–Cl > C–Br. The C–F bond dissociation energies in PFAS depend on the extent of fluorination of carbon atoms, the position of C–F bonds, and the nature of the head group in the molecule (Fig. 3).

In contrast, in chlorinated and brominated organic compounds, dissociation energies of C–X (X = Cl or Br) bonds depend on the degree of substitution at the carbon of the C–X bond. Thus, the strongest C–X bonds of chlorinated and brominated compounds are found in halogenated phenyls.[124]

Threshold limit values and response levels of common halogenated organic water pollutants

Threshold limit values (TLVs) serve as important benchmarks for monitoring workplace exposure. These values denote permissible airborne concentrations of chemical substances that the majority of workers can encounter in a repetitive manner throughout their career span, without detrimental health consequences. The American Conference of Governmental Industrial Hygienists (ACGIH) formulates TLV-time-weighted averages (TLV-TWAs) to safeguard against prolonged exposures, as well as short-term exposure limits to shield against sudden spikes in exposure. It is important to note that TLVs are not designed to establish a rigid demarcation between safe and hazardous exposures. Instead, their primary objective is to safeguard workers from potential health impacts.[125] The notification level is the concentration of a hazardous substance in the environment, above which specific actions or notifications are required. Notification levels are often used to assess water pollutants because they represent human health-based advisory levels for chemicals in drinking water, which lack maximum contaminant levels.[126] Human health-based advisory levels establish the contaminant concentration in drinking water, below which no adverse health effects and/or aesthetic impacts are expected during specific periods of exposure.[127] Actions might include reporting the presence of the substance to regulatory authorities or taking steps to mitigate the exposure or contamination. Notification levels are typically set by regulatory agencies and are designed to alert relevant parties when a certain level of contamination has been reached. In contrast, the response level represents a concentration of a hazardous substance in the environment that triggers specific actions or interventions to mitigate risks and protect human health or the ecosystem. Response levels are set to guide the appropriate measures to be taken when contamination reaches a certain level. These measures might include evacuation, containment, or clean-up, to prevent further exposure or harm.[126] TLVs and notification levels of common halogenated organic water pollutants that are discussed in this article are in Table 2.

Destructive remediation of chlorinated and brominated organic water pollutants

Destructive methods are necessary to treat waste streams or sludges after concentration of target pollutants by separation processes. Chlorinated and brominated organic pollutants can be destroyed by incineration,[157] non-thermal plasma discharge,[158] γ-irradiation,[159] biological, catalytic, photolytic, photocatalytic, or photochemical processes.

Table 2 Notification levels, response levels, and threshold limit values (TLVs) for common halogenated organic water pollutants in water unless otherwise noted; TLVs are for exposure averaged over an 8-hour work shift unless otherwise noted. Abbreviations of chemicals (in order of appearance): PFBA, perfluorobutanoic acid; GenX, hexafluoropropylene oxide dimer acid; PFDA, perfluorodecanoic acid; PFOS, perfluorooctane sulfonic acid; PFOA, perfluorooctanoic acid; Freon-11, trichlorofluoromethane; Freon-12, dichlorodifluoromethane; Freon-13, chlorotrifluoromethane; HCFC-22, chlorodifluoromethane; HCFC-142b, chloro-1,1-difluoroethane; HCFC-141b, 1,1-dichloro-1-fluoroethane; VC, vinyl chloride; DCE, 1,2-dichloroethane; PERC, tetrachloroethene; TCE, trichloroethene; 2,3,7,8-TCDD, 2,3,7,8-tetrachlorodibenzodioxin; PCB-47, 2,2′,4,4′-tetrachlorobiphenyl; PCB-77, 1,2-dichloro-4-(3,4-dichlorophenyl)benzene; BDE-47, 2,2′,4,4′-tetrabromodiphenyl ether; BDE-207, 2,2′,3,3′,4,4′,5,6,6′-nonabromodiphenyl ether; TBP, 2,4,6-tribromophenol; HBCD, hexabromocyclododecane; TBBPA, tetrabromobisphenol-A. Units: ppm (mg L^{-1}), ppb (μg L^{-1}), ppt (ng L^{-1}), ppq (pg L^{-1})

Class	Compound	Notification level	Response level	Ref.	Threshold limit value	Ref.
Fluorinated	PFBA	100 ppt	1000 ppt	128	5 ppt	129
	GenX	30 ppt	300 ppt	128	5 ppt	
	PFDA	20 ppt[a]	—	130	3 ppt	
	PFOS	6.5 ppt	40 ppt		4 ppt	
	PFOA	5.1 ppt	10 ppt		4 ppt	
	PFHxS	3 ppt	20 ppt		3 ppt	
Fluorinated–chlorinated	Freon-11	5 ppb[b]	150 ppb[b]	131	1000 ppm (airborne)	132
	Freon-12	1 ppm	10 ppm	133	1000 ppm (airborne)	134
	Freon-13	—	3000 ppm (airborne)	135	Not established	136
	HCFC-22	—	—		1000 ppm (airborne)	137
	HCFC-142b	—	—		1000 ppm (airborne)	138
	HCFC-141b	—	—		Not established	139
Chlorinated	VC	2 ppb	2 ppb	140,141	1 ppm (airborne)	142
	DCE	500 ppt[b]	500 ppt[b]	131	2 ppm (airborne)	143
	PERC	500 ppt[b]	5 ppb[b]	131	25 ppm (airborne)	144
	TCE	5 ppb[b]	500 ppt[b]	131	10 ppm (airborne)	145
	2-Chlorophenol	100 ppt (based on water aesthetics)	—	146	Not established	146 and 147
	2,3,7,8-TCDD	5 ppq[b]	30 ppq[b]		30 ppq	148
	PCB-47	500 ppt[b]	500 ppt[b]	131	1 ppb	149
	PCB-77	500 ppt[b]	500 ppt[b]	131	500 ppt	149
Brominated	BDE-47	—	24 ppt	150	50 mg kg^{-1} body weight per day	151
	BDE-207	—	—		50 mg kg^{-1} body weight per day	151
	TBP	—	—		Not established	152
	HBCD	—	—		100 mg kg^{-1} body weight per day	153
	TBBPA	—	15 ppb	154	10 ppb	155

[a] Massachusetts drinking water maximum contaminant levels, PFDA combined with other PFAS.[156] [b] California drinking water standards.[131]

Incineration. Incineration has been widely used to reduce the volume, potential infectious properties, and potential toxicity of waste.[160] This process burns the hazardous waste to carbon dioxide and water vapor, while also producing byproducts that are released as exhaust gas or remain as solid ash or soot.[160] Incineration has the advantage that large amounts of waste can be treated in a short period of time,[160] while additionally offering the possibility of providing heat energy to local communities;[161] however, incineration of halogenated pollutants does not always result in complete mineralization, which can give rise to the release of toxic emissions.[157] PCBs can be decomposed thermally; ergo, incineration at high temperatures can be employed for PCB destruction. PCBs are often formed as byproducts of lower-temperature municipal solid waste incineration.[157]

Non-thermal plasma and γ-irradiation. Non-thermal plasma treatment utilizes high-voltage electrical pulses to generate a corona discharge that excites electrons in the air to produce singlet oxygen, which reacts with water to generate ozone and hydroxyl radicals for pollutant destruction.[162] Gamma-irradiation utilizes γ-rays with sufficient energy, often from a ^{60}Co source, to ionize atoms, resulting in cleavage of molecular bonds, such as water, to create reactive radical species for pollutant destruction.[162] In addition to the inherent safety precautions and high-risk handling procedures of γ-rays, the efficiency of γ-irradiation relies on the extent which the radiation source has decayed, as that determines the deliverable dose. Non-thermal plasma has the advantage that the efficiency relies on electromagnetic generation of particles, which does not decay over time; however, its high energy demand creates inherent barriers for global use.[163,164] Non-thermal plasma discharge has been described for the degradation of PCB-77 (80% within 2 min) using a dielectric barrier discharge non-thermal plasma,[158] whereas PCB-47 was degraded by 70% within 60 min using pulsed corona discharge.[165] PCBs can also be decomposed with ionizing radiation in aqueous micellar solutions.[166] However, γ-radiation hazards originating from the required ^{60}Co γ-irradiation source must be mitigated.[167]

Chemical and biological techniques. Chemical and biological techniques make use of chemicals or microorganisms, respectively, to break down organic matter. Chemical processes are attractive destruction methods due to their simple operation; however, stoichiometric use of chemicals and associated production of sludge create large amounts of chemical waste, contributing to operational cost and complexity of separation.[168,169] Biological techniques have the advantage of

being self-sustaining processes, which result in less cost compared to methods requiring chemical additives or extensive maintenance. Nevertheless, biological processes require extended time for microbial growth, and the performance can suffer from inherent environmental factors, such as temperature or water composition.[169,170] Catalytic or oxidative processes have been reported for breakdown of chlorinated and brominated organic pollutants.[171,172] Biological processes have been applied to treat brominated water pollutants, such as anaerobic–aerobic processes for microbial degradation of tetrabromobisphenol-A.[173]

Electrochemical techniques. Electrochemical techniques utilize electrical energy to induce the mineralization of dissolved contaminants in water. Electrochemical systems offer many advantages, including operation at ambient temperature and pressure, no required auxiliary chemicals, and small footprint, making it an attractive technique for delocalized water treatment.[174] However, electrochemical technologies must be improved with regard to toxic by-products that result from inefficient mineralization, and with respect to electrode costs to enable adoption on an industrial scale.[174] Chlorinated and brominated organic water pollutants have been degraded by electrochemical processes.[25,175,176] Electrooxidative[176,177] and electroreductive[19,178,179] methods were used *via* direct electrocatalytic electron transfer or indirect interactions with electrochemically produced highly reactive transient species. We note that the production of toxic liquid bromine or chlorine gas is an inherent obstacle in electrooxidations of brominated or chlorinated water pollutants.[110,180–182]

Photo-assisted techniques. Photo processes and photo-assisted techniques utilize light absorption by molecules to directly dissociate target species or indirectly create reactive radical species in solution that carry out the degradation. Photo processes have several advantages, including operation at ambient temperature and pressure, low energy requirement, and no need for additional chemicals.[27] Nevertheless, current photo processes lack degradation and mineralization efficiency, resulting in by-product formation.[27] Methods involving illumination with light in the visible to vacuum ultraviolet range, such as direct photolysis or indirect photocatalytic and photochemical processes have been utilized for chlorinated and brominated pollutant mineralization.[183,184]

Sonolysis. Sonolysis utilizes the compression and expansion cycles of ultrasound waves that produce hot spots with high temperatures (approximately 5000 K) and pressures (approximately 1000 atm), due to cavitation bubble collapse.[185] In these hot spots, molecular bonds are cleaved directly through pyrolysis or indirectly through reactions with reactive radical species produced *via* pyrolysis.[185] Sonolysis is advantageous because no chemical additives are required and it is a simple process;[186,187] however, the localized production of high concentrations of reactive radical species is limited by recombination leading to inefficient degradation.[188] Direct pollutant destruction *via* sonolysis has been applied to remediate chlorinated and brominated water pollutants.[185,189–191] To enhance the degradation efficiency of sonolysis processes, auxiliary chemicals have been added to solutions that contained chlorinated or brominated pollutants.[189,192]

Recent progress in the destruction of chlorinated organic water pollutants

PCBs. Multiple PCBs were degraded *via* a combination of adsorption, photodegradation, and heterogeneous Fenton oxidation reactions, using a multifunctional magnetic β-cyclodextrin/graphitic carbon nitride catalyst (Fe_3O_4@β-CD/g-C_3N_4), with a degradation efficiency for different PCBs in wastewater ranging from 77% to 98%.[193] PCBs from transformer oil were photocatalytically degraded using carboxymethyl-β-cyclodextrin modified Fe_3O_4@TiO_2, with a degradation rate of PCBs of 83% after 16 minutes.[194] Dielectric barrier discharge non-thermal plasma degraded PCB77 in aqueous solution with a removal efficiency of PCB77 of 80% with helium as discharging gas and approximately 75% with oxygen as discharging gas.[158]

Dioxins. Dielectric barrier discharge in a lab-scale reactor degraded 2,3,7,8-TCDD in fly ash with a removal efficiency of 92%; this process was also used for degradation of other PCDD/Fs-containing fly ash, whose degradation efficiency depended on input energy and discharge time.[195] Another reported method to degrade 2,3,7,8-TCDD is use of extracellular fungal ligninolytic enzymes that were made of laccase enzymes. Ligninolytic fungus *Rigidoporus* sp. FMD21 degraded 2,3,7,8-TCDD by 77.4% in 36 days and produced 3,4-dichlorophenol.[196]

Tetrachloroethene (perchloroethylene, PCE). Degradation of PCE occurred under aerobic conditions using *Sphingopyxis ummariensis* bacteria in a gas-recycling fixed-bed bioreactor.[197] This process was more efficient with lower concentrations of PCE and achieved complete degradation of PCE in 25 hours.[197] PCE degradation using cobalt-mediated electroscrubbing with boron-doped diamond (BDD) coating supported on silicon or tantalum substrate anodes and stainless steel cathodes was reported.[198] The process worked by volatilizing of liquid PCE, followed by the treatment. BDD on silicon substrate anode reached a PCE removal efficiency of 75.7% in 2 hours, while BDD on tantalum substrate achieved a PCE removal efficiency of 90.5% in 2 hours.[198] Complete degradation of PCE was reported at pH 7 in 4 hours using nano-magnetite catalyzed with glutathione, with oxalic acid as the major by-product.[199]

Trichloroethene (TCE). Degradation of TCE by sodium percarbonate activated with Fe(II)-citric acid complex in the presence of surfactant Tween-80 has been described. At optimal conditions, 93.2% degradation efficiency was achieved in 15 minutes.[200] TCE was degraded using nanoscale calcium peroxide activated by Fe(II)/FeS, which enhanced generation of hydroxyl radicals, achieving 99.5% TCE removal efficiency in groundwater.[201] Polyvinyl alcohol coated nano calcium peroxide activated by Fe(II)/FeS or Fe(III)/FeS has been used to degrade TCE, with maximum degradation of 91% and 95% for Fe(II)/FeS or Fe(III)/FeS activated polyvinyl alcohol coated nano calcium peroxide, respectively.[202] Sequential anaerobic and aerobic treatment in the presence of the cyclic ether stabilizer 1,4-

dioxane degraded TCE. The anaerobic treatment used halorespiring consortium SDC-9 and effectively removed TCE, forming vinyl chloride (VC) and *cis*-dichloroethene (*cis*-DCE) as by-products. These by-products were removed along with the 1,4-dioxane during the subsequent aerobic bioaugmentation with *Azoarcus* sp. DD4.[203]

Other chlorinated organic water pollutants. Bimetallic zero-valent iron nanoparticles have been reported to degrade several chlorinated organic compounds, such as vinyl chloride (VC), 1,2-dichloroethene (DCE), TCE, and PCE. Bimetallic zero-valent iron nanoparticles with palladium and with nickel have completely degraded all compounds within 24 hours. VC, DCE, and TCE were completely degraded in 2 hours. PCE was degraded by about 97% and about 89% in 4 hours using Pd or Ni modified zero-valent iron nanoparticles, respectively, and complete degradation was achieved in 24 hours for both materials.[204] Degradation of chlorinated volatile organic compounds from contaminated groundwater was achieved by an O_3-bubble column reactor with a carrier-bound TiO_2/ultraviolet light system, with degradation efficiencies of 98% for *cis*-1,2-DCE, TCE and PCE and of 85% for trichloromethane without detectable by-product formation.[205] TCE and *cis*-1,2-DCE were degraded with *Cupriavidus* sp. CY-1 bacteria, whose growth was supplemented with TCE or *cis*-1,2-DCE and phenol or Tween 80 as a co-substrates. Use of CY-1 bacteria, whose growth was augmented by phenol, TCE and *cis*-1,2-DCE were converted into poly-β-hydroxybutyrate (PHB), which is a biodegradable plastic.[206]

Recent progress in the destruction of brominated organic water pollutants

Tetrabromobisphenol-A (TBBPA). Peroxymonosulfate in aqueous solution was activated by Ce, Sn, or Sb doped copper ferrite, $CuFe_2O_4$, catalysts prepared by a sol–gel combustion method, to degrade TBBPA.[207] A TBBPA removal efficiency of 90.1% in weakly basic conditions was achieved with Sb-doped $CuFe_2O_4$.[207] In another study, dielectric barrier discharge was used to completely decompose TBBPA in wastewater in 12 minutes, forming phenol, bisphenol A, catechol, hydroquinone, and 3,5-dibromophenol as by-products.[208] Bimetallic Co/Fe metal–organic frameworks/cellulose nanofiber membrane as a catalyst in a sulfate radical advanced oxidation process activated peroxymonosulfate and completely degraded TBBPA in 30 minutes at optimal conditions.[209]

2,4,6-Tribromophenol (TBP). An *in situ* peroxymonosulfate oxidation process with added chloride completely degraded TBP in salty wastewater, albeit with formation of undesired persistent halogenated products.[210] Ultraviolet photolysis of TBP in the presence of hydroxylamine achieved a debromination rate of 89.9% in 1 hour.[211]

Hexabromocyclododecane (HBCD). Near-complete aerobic biodegradation of aqueous HBCD was obtained by *Rhodopseudomonas palustris* YSC3 strain at 35 °C and neutral pH, forming bromide ions, pentabromodyclododecanol, and pentabromocyclododecene as by-products.[212] Isotope-labeled [^{13}C]-HBCD was efficiently mineralized in 5 days into $^{13}CO_2$ using organic montmorillonite-supported nanoscale zero-valent iron coupled with the bacterial strain *Citrobacter* sp. Y3.[213] HBCD removal and mineralization was obtained by an ultrasound-based advanced oxidation process, which completely degraded HBCD and accomplished 72% of total organic carbon removal in 40 minutes.[191] Complete degradation of HBCD was observed using nanoscale zero-valent aluminum in 8 hours in an ethanol/water solution at 25 °C, producing completely debrominated cyclododecatriene with 67% yield.[214] A ball-milled aluminum-carbon composite has been prepared to enhance the absorption and degradation of HBCD, completely absorbing HBCD in water in 1 hour and debrominating 63.44% of the pre-sorbed HBCD in 62 hours.[215] We note that zero-valent first-row transition metals or aluminum may oxidize in ambient aqueous conditions that are needed for global scalability.

2,2′,4,4′-Tetrabromodiphenyl ether (BDE-47). Reduction at zero valent zinc with cetyltrimethylammonium chloride surfactant achieved a BDE-47 removal efficiency of 98.6% in 1 hour, followed by a Fenton oxidation that decomposed all obtained debromination products into short-chain carboxylic acids that were mineralized in 2 hours.[216] Complete degradation of BDE-47 was achieved in 3 hours with a thermally activated persulfate system, forming one low-toxicity oxidation product.[217] A photocatalytic process using Ag/TiO_2 was developed for the degradation of BDE-47 in Triton X-100 surfactant solution under anaerobic conditions, predominantly producing diphenyl ether and the harmful bromodiphenyl ethers BDE-28, BDE-15, BDE-3,[218] which were found to be phytotoxic,[219] or exhibited hepatic[220] or reproductive toxicity[221] in mice. BDE-47 was degraded using a Fe(II)-catalyzed peroxymonosulfate activation process with the addition of gallic acid to accelerate the cycling of Fe, which enhanced peroxymonosulfate activation, reaching a degradation efficiency of 85% in 72 hours.[222] A functional bacterial consortium QY2 with an addition of methanol to enhance degradation efficiency and accelerate the debromination, hydroxylation, and phenyl ether bond breakage of BDE-47 completely removed BDE-47 in 7 days.[223]

Destructive remediation of fluorinated organic water pollutants including PFAS

The destructive remediation of fluorinated organic compounds, particularly PFAS, is an area of intense research. Methods for defluorination of the common PFAS chemical perfluorooctanoic acid (PFOA) have been reported by electrochemical reduction at a Rh/Ni cathode in dimethyl formamide *via* hydrodefluorination,[224] hazardous γ-irradiation with a ^{60}Co source in an alkaline solution under N_2-saturated conditions,[159] and mineralization of perfluorocarboxylic acids, including PFOA, *via* the formation of rapidly decomposing carbanions in polar, aprotic dimethyl sulfoxide electrolyte; the carbanion-based mechanisms can only operate in water-free, polar, aprotic solvent and fail to degrade sulfonic acid PFAS, such as PFOS.[225] Further, ^{19}F-NMR was used to quantify PFOA defluorination, which appeared to have a detection threshold of $\geq$5 mM (approx. 2000 ppm PFOA).[225] Globally scalable, viable technologies must work in aqueous media and

enable destruction of PFAS with much lower concentrations. Perfluorocarboxylic acids, such as perfluoro-butanoic, pentanoic, hexanoic, heptanoic, and octanoic acid (PFOA), were mineralized using a Ce-doped nanocrystalline PbO_2 film electrode;[226] the toxicity of lead poses challenges. While these reports are mechanistically intriguing, only cost- and energy-saving aqueous methods that utilize nontoxic, nonprecious materials and renewable electricity will be viable and sustainable on a global scale. Electrooxidation of PFOA and PFOS at Magnéli-phase Ti_4O_7 ceramic anodes outperformed mineralization at Ce-doped PbO_2 and Ti-modified boron-doped diamond electrodes, due to faster oxidation rate.[227] PFOA in water was degraded by ultraviolet-visible light assisted $Zn_xCu_{1-x}Fe_2O_4$-oxalic acid system, using a ferrite-based catalyst that allowed for magnetic catalyst recovery.[228]

Technoeconomic analyses of destruction techniques are indispensable to assess viability on a global scale. Significant research has been done to determine the most efficient destruction techniques.[27] Energy efficiency is important to lower operational costs and improve carbon footprints, whereas capital expenditures matter for assessing the affordability of units. Estimated energy and capital cost requirements of existing PFAS destruction techniques, based on literature data,[167,229–237] are shown in Fig. 4. Capital expenditure values refer to cost of equipment in the United States, are given in U.S. dollars, and are needed to treat at least one cubic meter of polluted water.

Incineration requires an initial investment of $41 938 050 for a one-line "turn-key" incineration plant.[83] The average amount of energy required for incineration is 0.45 kW h m^{-3} in the U.S., which has been measured and varies depending on the country and the type of incineration plant used.[233] The reported initial investment cost of γ-irradiation is $4 176 150, which includes the sum of the cost of the electron beam accelerator with lifespan of 15 years and personnel costs needed to run a γ-irradiation facility.[238] The equivalent electrical energy requirement to achieve 90% sulfadiazine degradation by γ-irradiation from a ^{60}Co source, taken here as a proxy for PFAS degradation, at a constant dose rate of 6.69 kGy h^{-1} has been reported to be 18 kW h m^{-3}.[239] The capital investment for non-thermal plasma[231,237] of $92 329 was obtained from a capital cost approximation for industrial wastewater plants.[163,240] The energy required to achieve a high removal rate of PFOA from water using non-thermal plasma is 100 kW h m^{-3}, which was deduced from the energy efficiency of non-thermal plasma setups.[237] Sonolysis by ultrasonication has a capital investment cost of $9 390 000, which has been calculated to include the part replacement cost, labor cost, analytical costs, chemical costs, and electrical costs.[230] The energy requirement for ultrasonication (1475 kW h m^{-3}) was calculated using the energy efficiency of ultrasonication in g $(kW\ h)^{-1}$.[235,241]

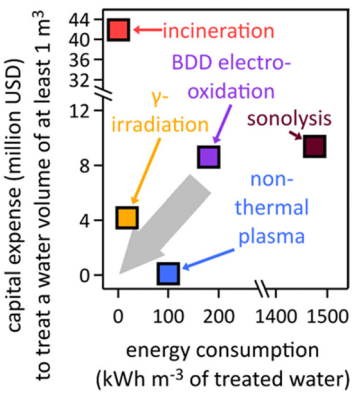

Fig. 4 Estimated electrical energy and capital expenditure requirements of existing PFAS destruction techniques, based on literature data;[167,229–237] BDD, boron-doped diamond. The grey arrow depicts the direction into which technologies must move in terms of capital expense and energy consumption to become viable on a global scale.

Chemical oxidation of PFOA by stoichiometric amounts of permanganate,[242] hydrogen peroxide, or persulfate[26,243] is cost-prohibitive and creates large amounts of chemical waste. Methods based on electrochemical processes have gained popularity because of lower energy demands than physical destruction methods, *i.e.* incineration, γ-irradiation, non-thermal plasma, and sonolysis. PFAS destruction by supercritical water oxidation[244] requires high initial investment;[245] we were unable to find numbers for investment costs. The thermal energy requirement for an efficient supercritical water generation facility is 5 MW for 250 metric tons of water per day.[246]

Electrooxidations of PFAS at expensive, often toxic, specialized anodes are nonviable.[226,235,247–257] The inter-electrode distance matters in electrolyzers because smaller distances are concomitant with less ohmic losses.[258] A generally accepted upper limit for inter-electrode distance in aqueous systems is 10 cm, which necessitates 10 m^2 geometric electrode area to treat 1 m^3 of polluted water,[258] rendering boron-doped diamond (BDD) electrodes cost-prohibitive.[259] At smaller inter-electrode distances, which generally result in higher electrocatalytic performance, the geometric electrode area requirement increases for treatment of a 1 m^3 batch, making the economics of BDD electrodes even more unfavorable. The energy required to halve an initial PFOA concentration of 15 mg L^{-1} with a BDD electrode of 38 cm^2 geometric area and an inter-electrode distance of 4 mm was reported as 180 W h L^{-1} at 50 mA cm^{-2}, for the treatment of 250 mL solution.[234] Conversion of these numbers to the treatment of 1 m^3 of polluted water requires BDD electrodes of 15.2 m^2 at a cost of $8.58 million[229] and 180 kW h m^{-3} electrical energy (Fig. 4). Electrochemical degradation of PFOA on ultrananocrystalline BDD coated on niobium electrodes additionally produced toxic perchlorate.[234] Ultraviolet-light-assisted electrochemical PFAS defluorination required cost-prohibitive platinum electrodes and N_2-saturated electrolyte.[260] Ergo, potentially viable PFAS destruction technologies must be more cost-effective and energy-saving to achieve economic feasibility and reduce carbon emissions.

Recent progress in the destruction of PFAS

Perfluorooctanoic acid (PFOA) has been degraded anaerobically to shorter chain perfluoroalkyl carboxylic acids and produced

fluoride in biosolids using *Acidimicrobium* sp. strain A6 and ferrihydrite.[261] PFOA has also been degraded efficiently by 80% over ball-milled boron nitride in deionized water or by 60% in simulated drinking water using photocatalysis for 2 hours.[262] The photocatalytic degradation of PFOA under UV-A and UV-C illumination with boron nitride was improved by using a composite of boron nitride and titanium oxide instead of neat boron nitride or titanium oxide. However, complete mineralization was not achieved and only shorter chain perfluorinated carboxylic acids were produced. The composite was capable of degrading PFOA by 68% in 7 hours using natural sunlight.[263] PFOA was degraded *via* a photocatalytic process that used a carbon-modified bismuth phosphate composite, absorbing PFOA in 2 hours and achieving nearly complete decomposition *in situ* in 4 hours under UV irradiation.[264] Another composite that has been developed for the photocatalytic degradation of PFOA in water is iron (hydr)oxides/carbon sphere (FeO/CS) composite. This material almost completely adsorbed PFOA in 1 hour, which subsequently underwent photodegradation and defluorination. During this process, PFOA was photodegraded by 95.2% and defluorinated by 57.2% in 4 hours.[265] Another photocatalytic process that used UV light and $Bi_3O(OH)(PO_4)_2$ in acidic conditions has been reported to degrade PFOA. However, this process was unable to degrade shorter chain PFAS unless some changes were made to the reactor system. With this system, challenges for implementation in real waters exist because the reaction was quenched by chloride and sulfate.[266] Complete defluorination of PFOA was achieved after 6 hours in water using a dual-frequency ultrasonic activated persulfate. This method can be used for other PFAS compounds, but not as effectively.[267] An electrochemical degradation process for PFOA using sodium sulfate has been developed, which enabled 99.5% degradation and 50% fluoride generation after 4 hours.[268] A sorptive photocatalyst Fe/TNTs@AC, which was based on activated carbon and titanium oxide, was synthesized and used for PFOA degradation. This catalyst completely absorbed PFOA in 1 hour, degraded it by 90% in 4 hours using UV radiation, and then mineralized 62% of the degraded PFOA to fluoride.[269] Another photocatalytic process that has been developed to degrade PFOA in aqueous solutions used In_2O_3 nanoparticles. This process worked most efficiently in acidic (pH = 2) conditions and successfully decomposed most of PFOA to fluoride and carbon dioxide within 90 minutes under UV irradiation, while also achieving 95.99% of PFOA defluorination.[270] Chemical mineralization of perfluorocarboxylic acids is mechanistically intriguing,[225] but works only in polar, non-protic electrolytes, such as dimethyl sulfoxide (DMSO), hampering global scalability, and fails to degrade sulfonic acid PFAS, such as PFOS.

Perfluorooctane sulfonic acid (PFOS) degradation has been reported, using sonolysis by 96.9%, 93.8%, and 91.2% at 400 kHz, 500 kHz, and 1000 kHz, respectively, in 4 hours.[271] Another method to degrade PFOS in an aqueous solution used reverse vortex flow gliding arc plasma; PFOS was degraded by 93.1% in 1 hour. This method can also be used to degrade other PFAS compounds, such as PFOA or PFDA and others.[272] Both PFOA and PFOS were defluorinated by 88% in 1 hour and 92% in 24 hours, respectively, using a UV light in a system that contained sulfite and iodide. Adding iodide to the UV light illuminated sulfite system greatly accelerated the defluorination of many PFAS. This system has achieved a complete removal of both PFOA and PFOS from concentrated mixtures in NaCl brine.[273] Electrooxidation using titanium suboxide anodes were used to degrade multiple PFAS compounds, such as PFOA and PFOS, whose concentrations decreased very quickly and approached zero in 1 hour.[274] Another method to degrade PFOA and PFOS as well as other PFAS compounds is γ-irradiation, using a ^{60}Co source. PFOS degradation was more efficient with branched PFOS isomers compared to linear molecules. Branched PFOS isomers were degraded almost completely, while PFOA was degraded by 87%.[275] A non-thermal plasma generator was custom-built to remove PFOA, perfluorohexanoic acid (PFHxA), and PFOS from water in both ultrapure and groundwater. In 30 minutes, PFOS was degraded completely in ultrapure water and by 85% in groundwater. PFHxA was degraded by 35% in ultrapure water and by 40% in groundwater, while PFOA degradation reached about 50% in both water systems.[276] PFOS and PFOA were significantly degraded in soil and groundwater by high dose electron beam technology. This process enabled the decrease of PFOS and PFOA concentrations in groundwater by 87.9% and 53.7%, respectively.[277] A duo-functional tri-metallic-oxide hybrid photocatalyst has been developed for the degradation of many PFAS compounds.[278] It possessed a high adsorption capacity and achieved 99.8% and 99.4% adsorption efficiency for PFOS and PFOA respectively, and it exhibited a high defluorination rate up to 67.6% for PFOS and 74.8% for PFOA. With this catalyst, PFOS was degraded by 95.5% in 5 hours, while PFOA was degraded by 98.9% in 30 minutes.[278] Boron-doped graphene sponge anodes have been reported for the degradation of PFAS compounds by electrochemical oxidation. This method had a higher removal efficiency for longer-chain than for short-chain PFAS, but its defluorination efficiency was lower than that of other methods.[279] GenX, which is a short-chain PFAS, was mineralized by an electro-Fenton process that paired a graphene-coated nickel foam electrode with a boron doped diamond electrode. This process achieved 92.2% mineralization after 6 hours of treatment.[280]

Aqueous advanced redox processes

Advanced oxidation processes, advanced reduction processes, and combined hybrid processes have emerged as promising strategies in water remediation due to potentially high organohalogen destruction efficiencies.[113,281] These processes can have rapid reaction rates, destroy pollutants without generating solid waste, do not require chemical oxidants, high pressures, or high temperatures, and can be powered by sustainable renewable electricity.[282–285] The advantages of advanced redox processes have led to intense research, such as photolytic, photochemical, photocatalytic, cavitation, electrochemical, and ionizing radiation approaches for water remediation, as well as combinations of these methods.[113]

Advanced oxidation processes (AOPs) generate and utilize highly reactive species with high oxidation potentials that are capable of cleaving carbon–halogen bonds of pollutants in wastewaters.[286] Oxidants are often radicals under aerobic conditions, such as the hydroxyl radical ($^{\bullet}OH$, aqueous lifetime 0.02 μs), superoxide radical anion ($OO^{\bullet-}$, aqueous lifetime 1.3 μs), sulfate radical anion ($SO_4^{\bullet-}$, aqueous lifetime 30–40 μs), and sulfite radical anion ($SO_3^{\bullet-}$), in addition to potent non-radical species, such as hydrogen peroxide (H_2O_2) and singlet oxygen ($^1O_2$, aqueous lifetime 3.5 μs).[285,287–301]

Advanced reduction processes (ARPs) produce highly reactive species with high reduction potentials to cleave carbon–halogen bonds of aqueous pollutants.[302] Reductants generated by ARPs require completely anaerobic conditions and are comprised of radicals, such as the sulfur dioxide radical anion ($SO_2^{\bullet-}$), sulfite radical anion ($SO_3^{\bullet-}$),[303] and hydrogen radical ($H^{\bullet}$), as well as non-radical hydrated electrons (e^-_{aq}, aqueous lifetime 0.43 or 8.6 μs at pH 7.0 or 9.5, respectively).[113,287,304] Oxygen-free conditions are often impractical, especially since the water oxidation half reaction can produce O_2,[305,306] membranes that separate oxidation and reduction half reactions cannot completely exclude oxygen crossover,[307] and airtight seals are inherently challenging on a large scale.

Mechanistic aspects of electrocatalytic aqueous advanced redox processes

A quantitative mechanistic understanding of aqueous advanced redox processes is lacking to date, albeit urgently needed to accelerate the development of viable aqueous electrocatalytic organohalogen destruction techniques. Radicals and reactive oxygen species play a major role in aqueous advanced redox processes, and the mechanisms of their formation and reactions with organohalogens must be understood in detail. Electrocatalysts significantly lower energy requirements for electrochemical transformations,[305] especially in aqueous systems, where potential-leveling by proton-coupled electron transfer (PCET) decreases needed energy inputs.[308]

Reactive oxygen species of the water–oxygen system

Aerobic aqueous processes that produce H_2O_2, $^{\bullet}OH$, $HOO^{\bullet}$, or $OO^{\bullet-}$ are based on the electrochemical transformations of the water–oxygen system (Fig. 5). Most of the transformations are electrochemical oxidations or reductions that proceed through energy-saving, potential-leveling PCET steps, which require that equal numbers of protons and electrons are transferred.[308]

Reactive oxygen species that are relevant for organohalogen destruction, *i.e.* H_2O_2, $^{\bullet}OH$, $HOO^{\bullet}$, and $OO^{\bullet-}$, can be produced directly or *via* H_2O_2 decomposition. Water oxidation can only produce O_2, H_2O_2, or $^{\bullet}OH$ through direct electrocatalysis. The one-electron-one-proton or two-electron-two-proton water oxidation reactions, given here together with standard potentials E^0 in V *vs.* the standard reference electrode (SHE), *i.e.* $H_2O \rightarrow {}^{\bullet}OH_{(aq)} + (H^+ + e^-)$, $E^0 = 2.38\ V_{SHE}$, or $2H_2O \rightarrow H_2O_2 + 2(H^+ + e^-)$, $E^0 = 1.76\ V_{SHE}$, are kinetically easier than the four-electron-four-proton reaction, *i.e.* $2H_2O \rightarrow O_2 + 4(H^+ + e^-)$, $E^0 = 1.23\ V_{SHE}$, but thermodynamically more uphill.[3] Molecular oxygen can be reduced to H_2O_2, $^{\bullet}OH$, $HOO^{\bullet}$, or $OO^{\bullet-}$ (Fig. 5).[309] Electrochemical reductions and oxidations that involve the transfer of less electrons and protons are kinetically faster than those that require the movement of more electrons and protons in the H_2O–O_2-system (Fig. 5). The electronic and chemical structures of intermediates of one-electron-one-proton transformations are known from computational density functional theory work, which cannot accurately capture concerted two-electron steps.[2,3,6] Together with the thermodynamic potentials below, these kinetic considerations allow as a function of electrolyte pH estimates which reactant species are likely formed in the highest concentrations for efficient destruction of halogenated organic water pollutants.

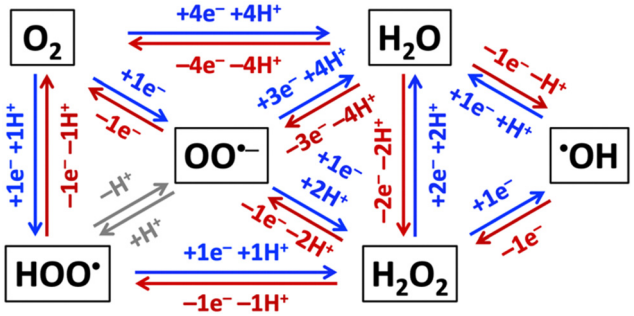

Fig. 5 Electrochemical reductions (blue) and oxidations (red) of non-surface-bound species in the H_2O–O_2-system.

Hydrogen peroxide is a precursor for $^{\bullet}OH$, $HOO^{\bullet}$, or $OO^{\bullet-}$ radical generation (Fig. 5) and, therefore, often called a pre- or pro-radical species. Hydrogen peroxide is a strong oxidant but reacts slowly with organics, so that it is often activated by alkali, activated carbon, heat, ultraviolet light, or transition metals,[296] such as iron-containing catalysts, which can in the presence of H_2O_2 serve as initiators for propagation reactions that generate $^{\bullet}OH$, $HOO^{\bullet}$, $OO^{\bullet-}$, and HO_2^- species *via* Fenton, Haber–Weiss, or photo-Fenton reactions.[310–313] Addition of H_2O_2 to the electrolyte was found to quench the production of toxic perchlorate at BDD electrodes.[314]

Thermodynamic potentials of reactive oxygen species

The thermodynamic potentials of reactive oxygen species determine their oxidation or reduction strengths in AOPs and ARPs of halogenated organic water pollutants. The protonation state and thermodynamic potential of aqueous reactive oxygen species depend critically on the electrolyte pH (Table 3). For example, at pH 0, $^{\bullet}OH$ and $HOO^{\bullet}$ are strong aqueous oxidants with standard potentials (*i.e.* thermodynamic potentials at pH 0) of 2.73 and 1.66, respectively, and both radicals possess sufficient thermodynamic driving force for PFAS oxidation. In contrast, at pH 14, the deprotonated hydroxyl radical anion ($O^{\bullet-}$) possesses a thermodynamic potential of 1.77 V, whereas the thermodynamic potential of the superoxide radical anion ($OO^{\bullet-}$) is only 0.65 V, which is insufficient to oxidize PFAS.

The protonation state of chemical species depends on their pK_a value and the pH of the aqueous solution; if the pH value is

Table 3 Reduction reactions of the O_2–H_2O-system and thermodynamic potentials E at pH 0, 7, and 14. From ref. 309, 315 and 316

Reduction reaction at pH 0	E (V) at pH 0	Reduction reaction at pH 7	E (V) at pH 7	Reduction reaction at pH 14	E (V) at pH 14
$O_2 \rightarrow HOO^{\bullet}$	−0.05	$O_2 \rightarrow OO^{\bullet -}$	−0.33	$O_2 \rightarrow OO^{\bullet -}$	−0.33
$O_2 \rightarrow H_2O_2$	+0.695	$O_2 \rightarrow H_2O_2$	+0.281	$O_2 \rightarrow HOO^-$	−0.065
$O_2 \rightarrow (H_2O +) {}^{\bullet}OH$	+0.73	$O_2 \rightarrow (H_2O +) {}^{\bullet}OH$	−0.31	$O_2 \rightarrow (OH^- +) O^{\bullet -}$	−0.03
$O_2 \rightarrow H_2O$	+1.229	$O_2 \rightarrow H_2O$	+0.815	$O_2 \rightarrow OH^-$	+0.401
$HOO^{\bullet} \rightarrow H_2O_2$	+1.44	$OO^{\bullet -} \rightarrow H_2O_2$	+0.89	$OO^{\bullet -} \rightarrow HOO^-$	+0.20
$HOO^{\bullet} \rightarrow (H_2O +) {}^{\bullet}OH$	+1.13	$OO^{\bullet -} \rightarrow (H_2O +) {}^{\bullet}OH$	+0.64	$OO^{\bullet -} \rightarrow (OH^- +) O^{\bullet -}$	+0.09
$HOO^{\bullet} \rightarrow H_2O$	+1.66	$OO^{\bullet -} \rightarrow H_2O$	+1.20	$OO^{\bullet -} \rightarrow OH^-$	+0.65
$H_2O_2 \rightarrow (H_2O +) {}^{\bullet}OH$	+0.80	$H_2O_2 \rightarrow (H_2O +) {}^{\bullet}OH$	+0.38	$HOO^- \rightarrow (OH^- +) O^{\bullet -}$	−0.03
$H_2O_2 \rightarrow H_2O$	+1.763	$H_2O_2 \rightarrow H_2O$	+1.349	$HOO^- \rightarrow OH^-$	+0.867
$^{\bullet}OH \rightarrow H_2O$	+2.72	$^{\bullet}OH \rightarrow H_2O$	+2.31	$O^{\bullet -} \rightarrow OH^-$	+1.77

Table 4 pK_a values of PFAS-relevant reactants and chemicals. From ref. 309 and 317–321

Species	pK_a	Ref.
$HOO^{\bullet}$	4.8	317
$^{\bullet}OH$	11.8	318
H_2O_2	11.6	319
H_2O	14.8	309
PFOA	2.5	320
PFOS	−3.27	320
$C_7F_{15}OH$	2.0	321

larger than the pK_a value of a species, the molecule is deprotonated. Aqueous pK_a values of reactants and chemicals that are relevant for PFAS destruction are shown in Table 4.

Mechanistic role of oxygen radicals for PFAS destruction

Reactive oxygen radicals, such as $^{\bullet}OH$, $O^{\bullet -}$, $HO_2^{\bullet}$, $OO^{\bullet -}$, are key species in AOPs and ARPs for C–C and C–F bond cleavage.[113,322] Superoxide radical anions ($OO^{\bullet -}$) can oxidize PFAS molecules; $OO^{\bullet -}$ can also act as a reductant and is the predominant species at pH > 5, as $HOO^{\bullet}$ has an aqueous pK_a of 4.8.[309] Hydroxyl radicals in aqueous solution are widely considered insufficient for PFOA or PFOS degradation[310,323,324] because $^{\bullet}OH$ radicals have an approximately 10× shorter aqueous diffusion distance than $OO^{\bullet -}$ radicals.[325,326] Quenching experiments with saturated alcohols that selectively scavenged solution $^{\bullet}OH$ radicals had no effect on the degradation of PFAS.[327,328] The exact role of $^{\bullet}O(H)$ radicals in aqueous electrocatalytic PFAS destruction is still debated. Recently, decreased degradation efficiency was observed in the presence of unsaturated allyl alcohol that is capable of quenching $^{\bullet}OH$ radicals in the vicinity of the anode, suggesting that adsorbed $^{\bullet}OH$ radicals played a significant role in PFAS degradation.[328,329] Adsorbed $^{\bullet}OH$ radicals are physisorbed; analog surface-bound species are non-radical hydroxide anions (OH^-) that lack the thermodynamic driving force for PFAS destruction.[309]

Auxiliary radicals and non-radical species

Addition of suitable solutes to aqueous media enables the formation of auxiliary radicals and non-radical redox agents in aqueous AOPs and ARPs. Reactive sulfur radicals are generated through dissociative reactions of persulfate, peroxomonosulfate, sulfate, or bisulfate to produce sulfate radicals, which are capable of assisting PFAS breakdown,[26,243,301,304] whereas the dissociation of bisulfite or sulfite anions produces sulfite radicals and hydrated electrons in strictly oxygen-free conditions.[113,301,330–332] Addition of iodide, dithionite, or ferrocyanide to anaerobic electrolytes can aid the detachment mechanism to produce hydrated electrons.[260,333] Dissociation of dithionite will produce reductive sulfur dioxide radicals.[302] Sulfite assists PFAS degradation through formation of persulfite.[323,334] Stoichiometric PFOA oxidation by permanganate has been observed.[242] Borate is known to react with H_2O_2, to produce peroxoborates that are stable at pH 8 to 12 and highly reactive towards nucleophiles.[335] Standard potentials of PFAS-relevant auxiliary species in aqueous solution are in Table 5.[285,288–299]

Mechanistically, the initial attack on the pollutant occurs by radical addition to a carbon–carbon double bond or by the abstraction of a carbon-bound hydrogen after the generation of auxiliary radicals and species.[336–338] In the case of perfluoro-compounds, such as PFOA and PFOS, that do not contain carbon-bound hydrogens and C=C double bonds, a different initial oxidation step is required that starts with the elimination of the head group in photo- or electrochemical processes.[282,339,340] An electron transfer from the carboxylic acid to the anode creates a carboxyl radical that undergoes decarboxylation to produce the carbon-centered perfluoroalkyl radical ($^{\bullet}C_nF_{2n+1}$) and CO_2.[176,183,274] Likewise, perfluorinated sulfonic acids are desulfonated *via* an analogue initial electron transfer.[256,282,341,342] The generated carbon-centered radicals quickly react with surrounding dissolved oxygen, water, or other radicals to form smaller carbonyl species. Once initiated, subsequent propagation reactions between the parent and

Table 5 Standard potential (E^0) of PFAS-relevant auxiliary species in aqueous solution. From ref. 285, 288, 291–296 and 298

Reaction	E^0 (V_{SHE})
$SO_4^{\bullet -} \rightarrow SO_4^{2-}$	2.44
$SO_3^{\bullet -} \rightarrow SO_3^{2-}$	0.73
$S_2O_8^{2-} \rightarrow SO_4^{\bullet -} + SO_4^{2}$	1.44
$SO_5^{\bullet -} \rightarrow SO_5^{2-}$	0.81
$H_2BO_3^- + 5H_2O \rightarrow BH_4^- + 8OH^-$ (pH 14)	−1.24
$MnO_4^- \rightarrow MnO_2$	1.70
$e^- \rightarrow e^-_{aq}$	−2.88
$H^+ \rightarrow H^{\bullet}$	−2.31

daughter species of the decomposing pollutant with highly reactive, strong oxidants will ultimately lead to complete mineralization of perfluorinated compounds.[286]

Reductive dehalogenation *via* hydrated electrons that are generated by ultraviolet photolysis from sulfite requires oxygen-free conditions, which are impractical on a large scale. Added sulfite can effectively deoxygenate aqueous solutions, forming sulfate, which in turn can form $SO_4^{\bullet-}$ for AOPs. Sulfite promotes the formation of $SO_3^{\bullet-}$, which is a mild oxidant[343] that reacts rapidly with oxygen to produce $SO_5^{\bullet-}$ and subsequently $SO_4^{\bullet-}$ and $^{\bullet}OH$ radicals, which are stronger oxidants and can more effectively degrade organohalogen pollutants.[301]

Electrocatalytic aqueous generation mechanisms of reactive species

Electrocatalytic AOP and ARP mechanisms proceed through direct electrocatalysis at materials surfaces,[96,115,283,344] indirect solution reactions,[176,345] or assisted reactions at materials and in solution.[332,346,347] In aqueous electrolyte without auxiliary solutes, aerobic electrocatalysis encompasses anodic water oxidation to H_2O_2 (precursor for AOPs), $^{\bullet}OH$ radicals (for AOPs), or O_2 (loss process),[3] and cathodic oxygen reduction at suitable catalysts[348,349] to H_2O_2, $^{\bullet}OH$ or $OO^{\bullet-}$ radicals, or water; H_2O_2 reduction to water can also occur (see Fig. 5 and 6A). Produced reactive species can diffuse into the bulk solution if they are sufficiently long-lived (see aqueous advanced redox processes) and react in indirect reactions to produce additional reactive species. The aqueous lifetime of $^{\bullet}OH$ is 0.02 μs, whereas that of $OO^{\bullet-}$ is 1.3 μs, resulting in a diffusion distance of $OO^{\bullet-}$ radicals (30 nm) that is approximately 10× longer than that of $^{\bullet}OH$ radicals (4.5 nm).[325,326] The diffusion distances of both $^{\bullet}OH$ and $OO^{\bullet-}$ radicals are too short for diffusion from electrodes into the bulk solution, but solution $^{\bullet}OH$ and $OO^{\bullet-}$ radicals can be created by decomposition of H_2O_2 in strongly acidic or alkaline water.[350,351] In the absence of dioxygen, *i.e.* in anaerobic media, anodic water oxidation produces $^{\bullet}OH$ radicals, H_2O_2, or O_2, which requires deoxygenation of the aqueous electrolyte, *e.g.* by sulfite,[343] to ensure completely oxygen-free conditions. Direct, unassisted cathodic electrocatalysis in anaerobic electrolyte consists of H_2O_2 reduction to water (Fig. 6B). Deep-ultraviolet light,[352] radiolysis,[297] or sonolysis[297] enable assisted electrocatalytic production of reactive oxygen radicals and, in O_2-free aqueous environment, hydrated electrons, e^-_{aq}, and hydrogen radicals, $H^{\bullet}$. Assisted aerobic electrocatalysis creates $^{\bullet}OH$ radicals, H_2O_2, or O_2 anodically by water oxidation, and H_2O_2, $^{\bullet}OH$, or $OO^{\bullet-}$ by

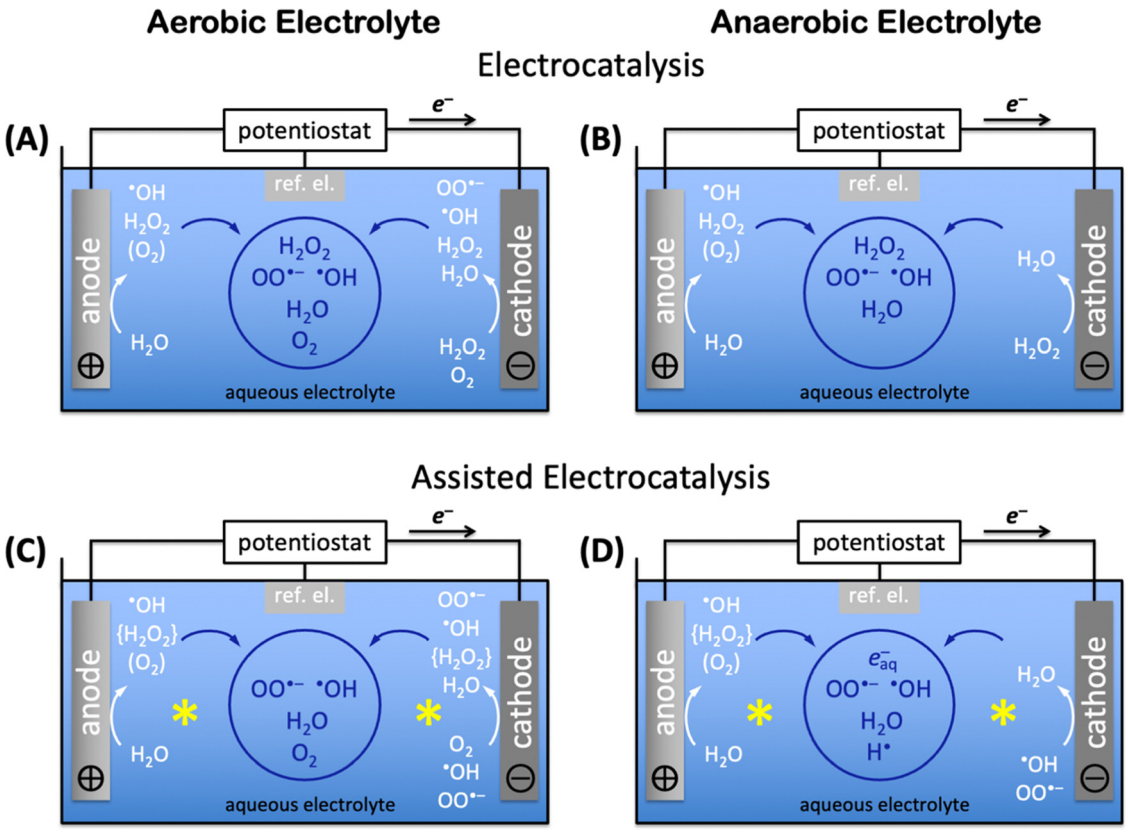

Fig. 6 Generation of radicals and reactive species in aqueous electrocatalysis for use in advanced redox processes; ref. el., reference electrode. Species produced at electrodes are in white, species produced in bulk solution are in blue in the blue circles; the yellow stars indicate assisting processes, such as deep ultraviolet light irradiation, radiolysis, or sonolysis. Anodic dioxygen (O_2) may be formed, depending on the water oxidation catalyst. Species in braces are short-lived intermediates. (A) Electrocatalysis in aerobic electrolyte, (B) electrocatalysis in anaerobic electrolyte, (C) assisted electrocatalysis in aerobic electrolyte, (D) assisted electrocatalysis in anaerobic electrolyte; e^-_{aq}, hydrated electron.

cathodic oxygen reduction; produced H_2O_2 immediately decomposes to $^{\bullet}OH$ radicals by deep-ultraviolet light,[352] or $^{\bullet}OH$ or $OO^{\bullet-}$ radicals by radiolysis[297] or sonolysis[297] processes that assist electrocatalysis (Fig. 6C). Assisted anaerobic electrocatalysis produces $^{\bullet}OH$ radicals, H_2O_2, or O_2 by anodic water oxidation (Fig. 6D). Elimination of O_2 to ensure anaerobic conditions and immediate decomposition of H_2O_2 to $^{\bullet}OH$ radicals by deep-ultraviolet light,[352] or $^{\bullet}OH$ or $OO^{\bullet-}$ radicals by radiolysis[297] or sonolysis[297] leave only $^{\bullet}OH$ radicals (or $OO^{\bullet-}$ radicals if radiolysis or sonolysis were used) as reducible species for the cathode half reaction (Fig. 6D); the highly energetic assisting processes continuously generate $^{\bullet}OH$ (or $OO^{\bullet-}$) radicals in the entire electrochemical cell, including in the vicinity of the cathode. Assisted anaerobic electrocatalysis (Fig. 6D) additionally enables the production of hydrated electrons, e^-_{aq}, and hydrogen radicals, $H^{\bullet}$, which are needed for ARPs, and which are only accessible in completely O_2-free aqueous electrolyte.

The aqueous generation mechanisms of reactive oxygen species and radicals are highly entangled, creating complex reaction networks. Much research has been dedicated to the elucidation of mechanisms. Pollutant degradation *via* AOPs and ARPs involves three principal steps: (i) reactive species generation, (ii) initial attack on the pollutant, and (iii) subsequential attacks on the pollutant until mineralization is complete.[113] Direct reactions occur at the electrode surface through electron transfers between the electrode and the chemical substrate.[283] In electrochemical oxidation reactions, the anodically generated holes must have sufficient electrochemical potential to create oxidizing agents, without turning on the four-electron-four-proton water oxidation electrocatalysis to dioxygen. Suppression of O_2 evolution requires applied potentials at or below the oxygen evolution potential, which is comprised of the thermodynamic potential and kinetic overpotential at the chosen pH conditions and catalyst materials.[96,305,306] Direct oxidation reactions are often slow because substrate adsorption at the anode controls the reaction rate. Due to these slow kinetics and limited useful applied anodic potential, direct electrocatalytic reactions typically do not result in complete mineralization of pollutants.[96]

Quasi-direct redox reactions occur at the electrode–electrolyte interface *via* physisorbed or chemisorbed redox species,[115,344] which are typically generated through reactions between the electrode and the aqueous electrolyte. Thus, the oxidizing strength in these processes is governed by the thermodynamic potential of the produced reactive species. Quasi-direct reactions have inherent mass transport limitations to and from the bulk solution because these processes must take place in the vicinity of the electrode–electrolyte interface.

Indirect processes occur in the bulk electrolyte, to where mediators migrate after electrochemical generation at the electrode–electrolyte interface, to react with pollutant species.[176,345] Reactive species for indirect AOPs and ARPs are typically long-lived to enable long diffusion distances into the bulk solution. Therefore, reactive oxygen species generated at the electrode–aqueous electrolyte interface are of limited use in these reactions due to their proclivity for recombination and short lifetimes despite being among the strongest oxidizing agents.[353] Some halogenated redox agents have longer lifetimes in comparison to those of reactive oxygen species, however, their selective reactivity and lower oxidation strength limits their reaction efficiency in the bulk electrolyte. Other advanced redox species, like sulfate radicals, possess longer lifetimes and simultaneously similar or greater oxidation strengths compared to reactive oxygen species, enabling indirect redox reations.[165,354,355]

Indirect processes have been coupled with other advanced redox activation processes to further increase the degradation efficiency of electrochemical systems.[332,346,347,356] Ultraviolet or visible light irradiation of electrochemical systems has most often been used. These coupled processes maintain similar reaction networks as dark electrochemical systems, with photoactivation of electrochemically generated mediators, so that increased concentrations of redox agents are produced at the electrode surface and within the bulk electrolyte.[332,346,347]

Photochemistry is frequently used to destroy pollutants and can be classified as three processes: photolysis, photochemical, and photocatalysis. Photo-assisted AOPs and ARPs have similar advantages as electrochemical processes, such as operation at ambient temperature and pressure, low operating costs, and no generation of waste streams.

Photolysis is the direct absorption of light by chemical substrates for direct degradation *via* homolytic bond scission or direct light absorption by water to produce highly reactive redox agents for indirect degradation.[113] The mechanism of photolysis consists of three steps: (i) light absorption that excites electrons in the molecule, (ii) primary photochemical processes that transform photoexcited molecules or result in relaxation back to the ground state, and (iii) secondary thermal reactions that transform the intermediates that were produced in step (ii).[357] Photolysis is limited to pollutants that exhibit large molar absorption cross sections and quantum yields, which restricts the overall applicability of photolysis.[358] Previous research has demonstrated applications of photolysis for pollutant degradation,[359–361] but photolysis is mainly used for the inactivation of pathogenic microorganisms.[362,363]

Direct ultraviolet photolysis of anaerobic water to form $^{\bullet}OH$ radicals, $H^{\bullet}$ atoms, and hydrated electrons, e^-_{aq}, (see Tables 3 and 5 for thermodynamic potentials) has been demonstrated with vacuum ultraviolet (VUV) wavelengths <200 nm, albeit with low quantum yields and very slow breakdown of PFAS.[364,365] Use of VUV irradiation is impractical because of the high absorption cross section of most materials at wavelengths below 200 nm. Deep ultraviolet irradiation at 254 nm is inefficient for direct photolysis of PFOA.[366] But deep ultraviolet light is capable of enhancing PFAS decomposition by AOPs of auxiliary chemicals (H_2O_2, SO_4^{2-}, SO_3^{2-}) *via* radical generation and indirect pollutant oxidation.[323,324,367]

Addition of transient chemical oxidants to water can overcome photolysis challenges and enhance the overall degradation efficiency of persistent pollutants[95,368] in a process known as photochemical degradation. Mechanistically, photochemical

processes proceed through similar pathways as photolysis, *i.e.*, photoactivation of transient chemicals to create highly reactive species, which then interact with pollutants and other molecules in the surrounding bulk electrolyte solution, creating complex reaction networks.[369] Typical oxidants in aqueous photochemical organohalogen destruction processes are H_2O_2, ozone, peroxosulfate, peroxomonosulfate, and sulfite.[113]

Photocatalysis employs a semiconductor catalyst to lower the activation energy required to photoactivate water and initiate AOPs and ARPs for pollutant degradation. Semiconducting photocatalysts for oxidation reactions must be n-type to take advantage of the band bending at the semiconductor–electrolyte interface to extract photogenerated holes that can perform oxidation reactions; conversely, photocatalysts for reduction reactions must be p-type to enable enhanced injection of photogenerated electrons into reducible species at the semiconductor–electrolyte interface. Band bending occurs under equilibrium conditions at the junction between a conductor and a semiconductor,[370–373] here the conducting electrolyte and the solid-state semiconductor photocatalyst. When a conductor and semiconductor are in contact, free electrons will transfer between the conductor and semiconductor because of the work function difference, to align the Fermi levels of both materials. The Fermi level, *i.e.*, the total electrochemical potential of electrons, can be considered as the hypothetical energy level of an electron. Under equilibrium conditions, a Helmholtz double layer forms at the conductor–semiconductor interface, where the conductor and semiconductor carry opposite charges near their surfaces due to electrostatic induction. A charge imbalance arises because semiconductors have a low concentration of free charge carriers; therefore, the electric field at conductor–semiconductor junctions cannot effectively be screened in the semiconductor, which causes the free charge carrier concentration near the semiconductor surface to be depleted relative to the bulk. This interfacial region is called the space charge region.[374] In n-type semiconductors, the Fermi level is closer to the conduction band than the valence band, and the electron concentration is larger than the hole concentration. Electrons are the majority charge carriers. Therefore, electrons are depleted in the space charge region, leading to excess positive charges, *i.e.* photoholes that can perform oxidations at the interface. In the space charge region, the energy band edges in the semiconductor are continuously bent upwards if the semiconductor work function is smaller than that of the adjoining conducting medium, *i.e.* the electrolyte. This happens due to the charge transfer induced by the electric field at the junction, and the effect is called band bending. Besides different Fermi levels at a semiconductor junction, an external electric field, adsorbed species, or surface states (due to termination of lattice periodicity of a material at the surface) can also induce band bending near the semiconductor interface.[374] Band bending can significantly decrease detrimental electron–hole pair recombination rates and enhance carrier transport to the semiconductor surface,[374] where redox reactions occur.

The general mechanism of photocatalysis starts with adsorption of light with a photon energy equal to or greater than the bandgap of the semiconductor to photoexcite an electron in the photocatalyst material from the valence band to the conduction band, leaving a hole in the valence band.[375,376] This photogenerated hole initiates oxidation reactions with the surrounding electrolyte to release reactive redox agents into the solution. Continually regenerated photo-holes and reactive species result in the oxidative destruction of pollutants.[375,377] Homogeneous and heterogenous photocatalytic processes have been reported for aqueous AOPs and ARPs. The most often used homogenous process is the photo-Fenton process, which employs iron complexes that undergo photochemical reduction to ferrous iron.[378] Ferrous iron catalyses H_2O_2 conversion to $^{\bullet}OH$ radicals.[378–380] This process is effective for persistent organic pollutant destruction,[378] but homogeneous processes suffer from inherent separation costs.[381–383] Heterogeneous photocatalysis employs solid catalyst materials that are readily recoverable and reusable, reducing separation expenses.[383] Halogenated organic pollutants have completely been mineralized to environmentally benign products, using photocatalysis.[376,384,385]

Advanced redox processes for chlorinated and brominated organic compounds

Brominated and chlorinated pollutants are often degraded cathodically *via* ARPs because oxidation of liberated bromide or chloride produces toxic liquid bromine or chlorine gas, respectively.[110,180–182] Nevertheless, Fenton-based AOPs have extensively been studied for the degradation of brominated and chlorinated pollutants. Fenton-based technology utilizes the reaction of ferrous ions with hydrogen peroxide, at an optimum pH, to generate hydroxyl radicals that react with pollutants in solution.[386] While Fenton-based methods are popular due to their wide application range, cost effectiveness of iron, strong anti-interference ability, simple operation, and rapid degradation,[387,388] significant disadvantages exist, such as the narrow working pH range and the generation of significant amounts of iron sludge.[389] Brominated flame retardants were completely mineralized,[390–392] whereas chlorinated trichloroethylene was not completely degraded.[393] Fenton methods in pyrite suspension have been developed to enhance reaction kinetics of H_2O_2 decomposition to $^{\bullet}OH$ radicals for more efficient pollutant degradation.[393] Iron ions activated persulfate anions to produce sulfate radicals in a Fenton-like reaction for the chemical degradation of trichloroethylene.[394] Photoelectrochemical systems have demonstrated enhanced AOP performance, synergistically degrading halogenated pollutants. Specifically, a photoelectrochemical system has been developed to degrade a series of chlorinated organic molecules to carbon dioxide, carbon monoxide, and chloride ions.[395] Pulsed potential electrolysis has been shown to significantly increase mineralization efficiencies compared to constant

potential electrolysis for chlorinated organic pollutants.[395] In a gas diffusion device, 4-chlorophenol and 4-bromophenol were electrochemically dehalogenated to phenol.[175]

Pairing Fenton processes with ultraviolet irradiation capitalizes on parallel reactive oxygen generation pathways. An ultraviolet-Fenton system achieved complete degradation of tetrabromobisphenol-A.[396] Hybrid Fenton-like processes have been paired with other AOPs and ARPs, such as sonolysis by ultrasound.[397,398] Hybrid systems have garnered much attention recently because of enhanced overall degradation rates. Sonophotocatalysis utilizes ultrasonic radiation and photocatalysis to synergistically generate more $^{\bullet}OH$ radicals than either individual method by itself does, evidenced by the degradation of 2-chlorophenol.[399] Hybrid systems that utilized ozone and H_2O_2 in a tube reactor nearly completely mineralized trichloroethylene and perchloroethylene in aqueous solution.[400]

Advanced redox processes for fluorinated organic compounds including PFAS

Conventional wastewater treatment processes are inefficient for PFAS destruction because of the exceptional stability of C–F bonds (see Table 1 and Fig. 3).[90] PFAS can be destroyed by AOPs and ARPs, particularly when aided by photo-assisted processes.[90] Direct photolysis is ineffective for treating many PFAS chemicals because the optical absorption of most PFAS molecules is limited to the UV-C region (<220 nm); UV-C irradiation requires specialized equipment and skin-cancer safety precautions; system lifetimes were inherently lower than those of systems irradiated with longer wavelengths, adding to overall capital investments.[90] Photocatalysis enhanced PFAS degradation, as was reported for 254 nm (deep ultraviolet) illumination of the benchmark photocatalyst TiO_2 for PFOA decomposition; irradiation with 315–400 nm light significantly decreased degradation performance, suggesting that the ability of the photocatalyst to generate sufficiently strong oxidants, such as $^{\bullet}OH$ or $OO^{\bullet-}$, controlled defluorination efficiency.[401] Addition of persulfate to aqueous systems increased PFAS defluorination from negligible to nearly complete mineralization, *via* direct photolysis of persulfate to sulfate radicals.[402–404] Photo-assisted electrochemical processes demonstrated enhanced degradation efficiencies of fluorinated compounds compared to dark electrochemical processes.[260,341,405,406] The photo-Fenton process was utilized to increase transient radical concentrations compared to those generated by the dark Fenton process[407] and concomitantly enhanced PFAS degradation.[408] Addition of auxiliary chemicals to the electrochemical system benefitted the overall degradation efficiency of PFAS chemicals.[280,330] Direct electrochemical and indirect hybrid electrochemical systems have been investigated for fluorinated pollutant degradation.[234,260,280,330,339,341,405,406,409,410] Reported direct electrochemical PFAS degradation processes were most efficient when they occurred on boron-doped diamond (BDD) electrodes,[234,339,409,410] which are cost-prohibitive on a large scale (see Fig. 4).

Mechanisms of electrochemical aqueous PFAS destruction

All PFAS electrooxidation pathways start with a direct electron transfer to the anode, which is rate-limiting according to density functional theory calculations,[282] followed by decarboxylation (perfluorinated carboxylic acids, such as PFOA)[176,183,274] or desulfonation (perfluorinated sulfonic acids, such as PFOS)[256,282,341,342] to form a $^{\bullet}C_nF_{2n+1}$ radical, from which CF_2 moieties are unzipped by $^{\bullet}OH$ or $OO^{\bullet-}$ radicals to form shorter-chain perfluoroalkyl radicals, ultimately producing CO_2 and HF, which can safely be mineralized as calcium-containing solids.[411] Several reaction pathways have been proposed, depending on the chemical nature of the oxidant (Fig. 7).[304,310,412] All reported mechanisms of aqueous electrochemical degradation of PFOA start with electron transfer to the anode and decarboxylation, liberating CO_2, to form the $^{\bullet}C_7F_{15}$ radical, which then further reacts with $^{\bullet}OH$ to form $C_7F_{15}OH$ in the hydroxyl radical mechanism or with oxygen and protons in the hydrogen peroxide mechanism.[304,310,412] Other auxiliary anions in aqueous solution, such as sulfate or borate, enhance the generation of superoxide radial anions or hydroxyl radicals, opening pathways that proceed through the hydrogen peroxide mechanism or hydroxyl radical mechanism, respectively (Fig. 7A). The intermediate $C_7F_{15}OH$ (structurally equal to $C_6F_{13}CF_2OH$) is unstable and undergoes intramolecular rearrangement and hydrolysis, by which $C_6F_{13}COO^-$ is produced, effectively unzipping one CF_2 moiety as one CO_2 and two HF molecules from the original $C_7F_{15}COO^-$ reactant.[304] Alternatively, the $^{\bullet}C_7F_{15}$ radical can react with dioxygen in the oxygen mechanism (Fig. 7A) to form the $C_7F_{15}OO^{\bullet}$ radical, followed by decomposition of $C_7F_{15}O^{\bullet}$ to perfluoorohexyl radical and carbonyl fluoride.[412]

Reported aqueous electrochemical degradation of PFOS starts with a direct electron transfer to the anode. Because the bond dissociation energy of the C–S bond (272 kJ mol^{-1}) in PFOS is lower than that of the C–C bonds (346 kJ mol^{-1})[415] or that of the C–F bonds (464.5–481.5 kJ mol^{-1}),[416] desulfonation occurs after the initial electron transfer (mechanisms I and III).[412–414] Nevertheless, mechanism II has been proposed, which unzips CF_2 moieties before desulfonation.[412] Desulfonation can follow different mechanistic pathways (Fig. 7B). In mechanism I, the initial electron transfer to the anode is followed by the formation of a very unstable $^{\bullet}C_8F_{17}SO_3^-$ radical that reacts with water to form $^{\bullet}C_8F_{17}$, which undergoes hydroxylation and hydrolysis reactions to form deprotonated PFOA and HF. This cycle repeats seven times to produce CO_2 and HF.[413,414] In the presence of hydrogen radicals ($H^{\bullet}$), aqueous electrocatalytic PFOS degradation follows mechanisms II or III, where PFOS ($C_8F_{17}SO_3^-$) reacts upon electron transfer with $H^{\bullet}$ under fluoride abstraction, to form $C_8HF_{16}SO_3^-$, which reacts further with $^{\bullet}OH$ radicals to form $^{\bullet}C_8F_{16}SO_3^-$ and water. We note that $H^{\bullet}$ radicals only exist under anaerobic conditions (Fig. 6). In mechanism II, the intermediate $^{\bullet}C_8F_{16}SO_3^-$ reacts with $^{\bullet}OH$ radicals, undergoes hydrolysis and decarboxylation reactions, to form $C_7F_{15}SO_3^-$ upon liberation of $CO_2^{\bullet-}$, whose

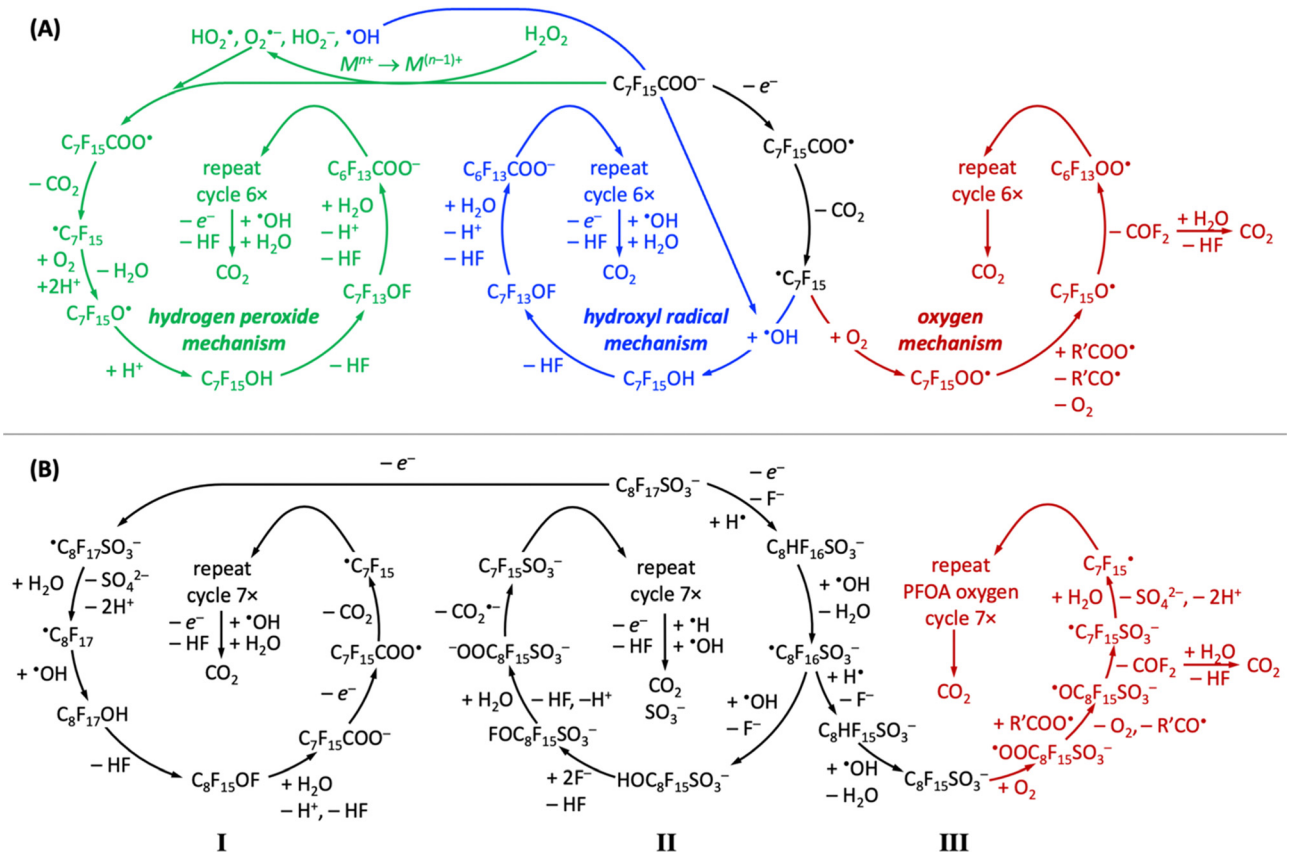

Fig. 7 Overview of reported proposed reaction pathways of electrochemical aqueous oxidation of PFOA (A) and PFOS (B), adapted from ref. 304, 310 and 412 (PFOA) and ref. 412–414 (PFOS).

spectroscopic signature is known,[417] and the cycle repeats seven times until only CO_2, HF, and SO_3^- remain of PFOS. In contrast, in mechanism III, the intermediate $^{\bullet}C_8F_{16}SO_3^-$ undergoes an H/F exchange and a decarboxylation reaction to form $^{\bullet}C_7F_{15}$, which is an intermediate of aqueous electrocatalytic PFOA degradation (Fig. 7A). In mechanism III, PFOS-derived $^{\bullet}C_7F_{15}$ has been reported to decompose along the oxygen mechanism pathway of PFOA until CO_2 and HF are obtained as final products (Fig. 7B).[412] Likewise, $^{\bullet}C_7F_{15}$ decomposition can also proceed through the PFOA hydroxyl radical mechanism to arrive at the desired products CO_2 and HF.

Carbon-based radicals are longer-lived than oxygen-based radicals;[418] in aqueous electrolyte, carbon-based radicals are at PFAS molecules, and oxygen-based radicals are the reactive oxygen species that stem from electrolytes. The protonation state, which depends on electrolyte pH and pK_a values of reactants and intermediates (see Table 4), critically affects mechanistic pathways. For example, the $C_7F_{15}OH$ intermediate of the hydrogen peroxide and hydroxyl radical mechanisms in Fig. 7A can only be formed at pH values below 2 (see Table 4).

Future research directions

More research is needed to develop viable, globally scalable technologies for the destruction of halogenated organic water pollutants. Systems must work in aqueous media, consist of nonprecious materials, minimize capital expenditures and energy requirements, and be capable of being powered by renewable electricity for sustainability. A quantitative mechanistic understanding of organohalogen destruction *via* aqueous advanced redox processes is urgently needed, for which analytical detection methods for organohalogens and transient species must be improved, and the development of new catalysts and processes must be advanced.

Analytical PFAS detection methods

Detection of low concentrations of organohalogens in the ppb to ppt range is challenging, particularly in natural water samples, in which ubiquitous abundant ions, such as chloride, can interfere.[419,420] Defluorination performance is typically assessed by fluoride ion quantification by ion selective electrode measurements.[421] Nuclear magnetic resonance (NMR) spectroscopy has been used since the early 1960s to detect PFOA and PFOS, with a limit of detection of 1.5 μM at that time.[422] Gas chromatography (GC) and liquid chromatography (LC) have gradually gained more importance as separation techniques prior to compound identification and quantification. GC can only separate neutral and volatile analytes with low molecular weight, and is limited by low sensitivity and long separation times.[423,424] Compared to GC, LC is more widely utilized in quantitative organohalogen analysis, owing to its

ability to separate semi- or non-volatile, polar, higher molecular weight, and thermally unstable compounds.[47] A widely used analysis technique is LC coupled with mass spectrometry (LC-MS) to detect halogenated contaminants,[425] which is often used together with reference standards that are currently available for one hundred of the hundreds of potentially relevant PFAS that are harmful to human health.[426] High-resolution mass spectrometry (HRMS) has emerged as a key tool for identifying legacy and novel PFAS. HRMS can detect more than 750 PFAS.[427] LC and GC, coupled with various HRMS-based techniques, have been widely used for the identification and quantification of organohalogens.[428] LC/GC-HRMS has extremely high selectivity, high resolving power, and is capable of detecting unknown PFAS. The lowest limit of PFAS detection for LC/GC-HRMS that has been reported was 100 nM.[429] The high cost of HRMS instrumentation and challenges with respect to differentiation of PFAS isomers are the main disadvantages of LC/GC-HRMS.[26] PFAS concentrations down to 10 nM are detectable by mobility spectrometry combined with LC and MS, which provides high selectivity and sensitivity as well as fast detection, but is expensive and unable to distinguish PFAS isomers, which limits broad usability.[430]

Catalyst development

The development of new, nonprecious, efficient, selective, and robust catalysts is critical for the advancement of halogenated pollutant destruction. Catalyst materials are the foundation of degradation technologies because catalysts lower kinetic barriers in the conversion of supplied energy into chemical energy that initiates the degradation process. New synthetic and computational methods are needed to advance the design of robust, active, selective, and globally scalable catalysts, predicated on a quantitative mechanistic understanding.[6,16,17,305,306,431–435] Advanced *operando* spectroscopies are essential to reveal the electronic and physical structures of catalysts under turnover, which together with catalyst property–performance relationships will accelerate catalyst discovery through rational design.[435–441] Understanding how surface species bind to catalysts through first principles and machine learning computations is key to inform and direct experimental investigations in the vast materials space.[442,443]

The electronic and geometric structure of catalysts, including changes during turnover and bonding motifs of reaction intermediates can be determined by advanced *in situ* or *operando* spectroscopies, combined with first principles and machine learning. *In situ* techniques monitor changes of the catalyst material under turnover, whereas *operando* spectroscopies additionally identify and quantify generated products during catalysis, thus enabling direct catalyst property–performance relationships during catalytic cycling. *In situ* and *operando* spectroscopies are often employed to gain a mechanistic understanding of electron, ion, and mass transport at catalyst interfaces,[444] providing insights into the surface and bulk structure of catalysts, their composition, oxidation states, and adsorbed intermediates under reaction conditions.[436,441,445] *In situ* and *operando* spectroscopies additionally enable critical insights into reaction pathways,[446] especially when coupled with computational studies.

Some of the most frequently used *in situ* and *operando* characterization techniques of catalyst materials are *in situ* Raman and surface enhanced Raman spectroscopy (SERS),[445,447] Fourier transform infrared spectroscopy (FTIR),[446] and the synchrotron-based techniques X-ray diffraction,[446] X-ray absorption spectroscopy,[448] near ambient pressure X-ray photoelectron spectroscopy,[446] high-energy-resolution fluorescence-detection X-ray absorption spectroscopy,[449] and X-ray absorption fine structure spectroscopy,[449] sometimes used in grazing incidence angle configuration to enhance catalyst surface specific information.[450] To gain a more accurate and quantitative understanding of catalysts and to reveal critical insights into the thermodynamics and kinetics of species during electrocatalysis, theoretical approaches, such as first principles density functional theory (DFT) calculations and microkinetic modelling simulations are often combined with *in situ* and *operando* characterization techniques.[436,444,451,452] First-principles calculations, rooted in quantum mechanical electronic structure theory, have been utilized to analyse the intimate and dynamic relation between the microscopic processes and the meso- to macroscopic environment.[453] DFT is the most commonly used first-principle method and utilizes functionals of spatially dependent electron density calculations to investigate the electronic structure of atoms, molecules, and solids.[454] First-principle calculations are especially important in the context of catalyst discovery because they enable screening for new catalysts based on user-defined criteria and hypotheses, such as optimal activity, stability of elements under specific conditions, formation energy, selectivity, and material phases.[2,455] These computational screening tools have been employed to analyze ensemble effects and electronic effects, to determine catalytic activity and selectivity.[455] Electronic effects control the binding of the reaction intermediates.[455] DFT calculations can be used to predictively design advanced catalysts, utilizing functional mechanisms of existing catalysts, comparing them, and making predictions which of these mechanisms is most suitable for each future reaction.[442,455] Theoretical predictions from first-principle calculations are based on properties calculated from basic physical quantities and do not consider experimental results. Thus, it is challenging to quantitatively understand catalysts by advanced *in situ* or *operando* spectroscopies or theoretical models alone. Therefore, experimental results and theoretical models are nowadays often combined with machine learning algorithms that enable a better understanding of the nature of chemical bonding and its variation in strength across physically tuneable factors.[442] Data-driven artificial intelligence models are capable of being integrated into active and iterative learning schemes that incorporate experimental results to improve the extrapolative, *i.e.*, predictive, capabilities of models.[456,457] Machine learning can also be combined with multi-scale simulations and quantum mechanics to predict the performance of surface sites of catalysts.[458]

Advanced *in situ* or *operando* spectroscopies, together with computational first principles and machine learning

approaches enable much-needed quantitative understanding of catalytically active sites, reactions centres, and reaction mechanisms.[446,451,458,459] Right now, detailed DFT calculations and machine learning studies have challenges, such as high computational cost and potential loss of physical intuition since most models consist of complicated mathematical formulations that are difficult to interpret.[442] Furthermore, reporting of experimental and computational information in much detail must be ensured to overcome challenges regarding choosing suitable functionals in DFT calculations.[460,461] Multi-disciplinary approaches that combine experimental electrochemical performance assessments, *operando* spectroscopies, and computational approaches have to date the greatest potential to advance catalyst development.[451]

Process development

The thermodynamics, kinetics, mass transport, and chemistries of a system (*i.e.* the four pillars of chemical engineering) govern the overall electrocatalysis process and are tunable by the electrocatalytic process parameters outlined in Fig. 8. The electrolyte pH critically affects the thermodynamic potentials and chemistries, including generation mechanisms and protonation state, of reactive species produced during catalytic turnover (see Table 3). Electrolytes composed of small ions enhance mass transport, and electrolyte composition affects chemistries, particularly with respect to auxiliary solutes that can form transient radicals with high oxidation or reduction strengths. The electrolyte temperature impacts kinetics and mass transport of the system. The reaction time influences reaction kinetics, and electrolyte agitation increases mass transport. The applied potential controls the thermodynamics, kinetics, and chemistries by making different mechanistic pathways accessible.

The scaleup of halogenated pollutant destruction technologies from the laboratory scale to industrially relevant scales demands that investigated systems are operated in water at pollutant concentrations that occur in the field, or at least at concentrations that are achievable by separation techniques,[462,463] necessitating optimization of substrate mass transport.

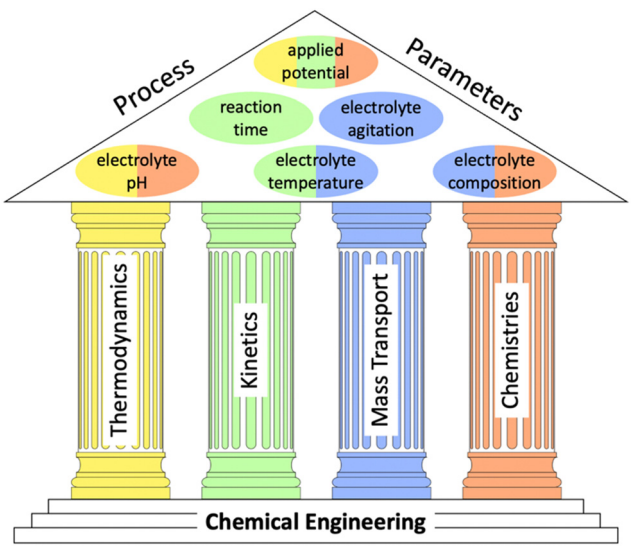

Fig. 8 Electrocatalytic process parameters, color-coded to visualize which chemical engineering descriptor they affect.

Detection of transient ARP and AOP species

Quantitative analytical techniques are needed for the detection of short-lived, highly reactive redox species[352,464–466] that are produced during assisted or unassisted electrocatalytic ARPs and AOPs, to develop a quantitative mechanistic understanding of organohalogen destruction processes. Electron paramagnetic resonance (EPR) spectroscopy is the premier method for radical detection.[467–469] Freeze or spin trapping preserves radical species long enough to detect them in an EPR spectrometer.[335] Spin traps are chemicals that react with radicals to create longer-lived, paramagnetic, EPR-active species, which are used to identify radicals with short lifetimes.[335] Qualitative radical identification is important for understanding which species are involved in ARP and AOP mechanisms. Nevertheless, quantification is necessary to deeply understand mechanisms, and optimize reaction conditions and overall pollutant degradation. While EPR is typically used for identification of radical species, an external standard, such as 2,2,6,6-tetramethylpiperidine 1-oxyl (TEMPO), can be utilized to obtain quantitative data.[470] Other quantitative detection methods are fluorescence and optical spectroscopy that utilize turn-on or turn-off dyes to determine radical concentrations.[352,471,472] These dyes typically react directly with radical intermediates, resulting in a change in the fluorescence or absorption spectrum of that dye, enabling the determination of concentrations of radical intermediates. Faster, more cost-effective, and more sensitive detection methods must be developed to accelerate the innovation of viable aqueous electrocatalytic organohalogen destruction techniques.

Conclusions

Halogenated organic compounds are widespread due to their exceptional utility and because they were initially considered nonmetabolizable and nontoxic, owing to the extreme stability of carbon–halogen bonds. However, prolonged use has led to their accumulation in the environment and organisms globally. We have introduced various classes of these pollutants categorized by halogen type (fluorine, chlorine, bromine), discussed important policies and regulations, outlined their applications, and highlighted associated environmental and human health risks. We discussed remediation techniques, focusing on carbon–halogen bond strengths, capital expense and energy needs for destruction, and electrocatalytic aqueous advanced redox processes. We highlighted mechanistic details of electrocatalysis, including oxidations and reductions of the water–oxygen system, as well as thermodynamic potentials, protonation states, and lifetimes of radicals and reactive oxygen species in aqueous electrolytes, importantly, at different pH conditions.

We pointed out that advanced reduction processes necessitate anaerobic conditions, which are impractical beyond the laboratory scale because electrocatalytic water oxidation can produce dioxygen, membranes partitioning oxidation and reduction half-reactions cannot completely prevent oxygen crossover, and airtight seals are inherently challenging in large-scale applications; ergo, advanced oxidation processes appear to be more promising. We reviewed aqueous advanced redox processes for different halogenated compounds and PFAS (per- and polyfluoroalkyl substances), detailing potential mechanisms. Future research directions require quantitative understanding of destruction mechanisms, improved detection methods, advanced catalyst development, and energy-efficient processes. Scalable systems using nonprecious materials, powered by renewable electricity, are crucial. We outlined the interconnectedness of electrocatalytic process parameters and their effect on the chemical engineering descriptors thermodynamics, kinetics, mass transport, and chemistries, all vital in steering complex reaction networks. Finally, we suggested strategies to accelerate the development of effective aqueous electrocatalytic techniques for organohalogen destruction.

Abbreviations

ACGIH	American Conference of Governmental Industrial Hygienists
AOP	Advanced oxidation process
ARP	Advanced reduction process
BDD	Boron-doped diamond
BDE-15	4,4′-Dibromodiphenyl ether
BDE-207	2,2′,3,3′,4,4′,5,6,6′-Nonabromodiphenyl ether
BDE-22	2,3,4′-Tribromodiphenyl ether
BDE-28	2,4,4′-Tribromodiphenyl ether
BDE-3	4-Monobromodiphenyl ether
BDE-47	2,2′,4,4′-Tetrabromodiphenyl ether
BFR	Brominated flame retardant
CFC	Chlorofluorocarbon
CFC-11	Trichloro(fluoro)methane
CFC-12	Dichlorodi(fluoro)methane
CFC-13	Chloro(trifluoro)methane
CIPAH	Chlorinated polycyclic aromatic hydrocarbon
DCE	1,2-Dichloroethane
decaBDE	Decabromodiphenyl ether
DFT	Density functional theory
DMSO	Dimethyl sulfoxide
e-waste	electronic waste
EPR	Electron paramagnetic resonance
Freon-11	Trichloro(fluoro)methane
Freon-12	Dichlorodi(fluoro)methane
Freon-13	Chloro(trifluoro)methane
Fs	Furans
FTIR	Fourier transform infrared spectroscopy
GC	Gas chromatography
GenX	Hexafluoropropylene oxide dimer acid
HBCD	Hexabromocyclododecane
HCFC	Hydrochlorofluorocarbon
HCFC-141b	1,1-Dichloro-1-fluoroethane
HCFC-142b	Chloro-1,1-difluoroethane
HCFC-22	Chloro(difluoro)methane
HFC	Hydrofluorocarbon
HRMS	High-resolution mass spectrometry
LC	Liquid chromatography
MS	Mass spectrometry
NMR	Nuclear magnetic resonance
octaBDE	Octabromodiphenyl ether
PBB	Polybrominated biphenyl
PBDD	Polybrominated dibenzo-*p*-dioxins
PBDE	Polybrominated diphenyl ethers
PCB	Polychlorinated biphenyls
PCB-47	2,2′,4,4′-Tetrachlorobiphenyl
PCB-77	1,2-Dichloro-4-(3,4-dichlorophenyl)benzene
PCDD	Polychlorinated dibenzo-*p*-dioxins
PCDF	Polychlorinated dibenzofuran
PCE	Perchloroethylene = tetrachloroethene
PCET	Proton-coupled electron transfer
pentaBDE	Pentabromodiphenyl ether
PERC	Tetrachloroethene
PFAS	Per- and polyfluoroalkyl substances
PFBA	Perfluorobutanoic acid
PFDA	Perfluorodecanoic acid
PFHxA	Perfluorohexanoic acid
PFOA	Perfluorooctanoic acid
PFOS	Perfluorooctane sulfonic acid
PHB	Poly-β-hydroxybutyrate
ppb	Parts per billion ($\mu g\ L^{-1}$)
ppm	Parts per million ($mg\ L^{-1}$)
ppq	Parts per quadrillion ($pg\ L^{-1}$)
ppt	Parts per trillion ($ng\ L^{-1}$)
R-11	Trichloro(fluoro)methane
R-12	Dichlorodi(fluoro)methane
R-13	Chloro(trifluoro)methane
SERS	Surface-enhanced Raman spectroscopy
TBBPA	Tetrabromobisphenol-A
TBP	2,4,6-Tribromophenol
2,3,7,8-TCDD	2,3,7,8-Tetrachlorodibenzodioxin
TCE	Trichloroethene
TEMPO	2,2,6,6-Tetramethylpiperidine 1-oxyl
TLV	Threshold limit value
TWA	Time-weighted average
UV	Ultraviolet
VC	Vinyl chloride
VUV	Vacuum ultraviolet

Author contributions

Madeleine K. Wilsey, writing – original draft preparation, writing – review and editing, visualization; Teona Taseska, writing – original draft preparation, visualization; Ziyi Meng, writing – original draft preparation; Wanqing Yu, writing – original draft preparation; Astrid M. Müller, conceptualization, writing – original draft

preparation, writing – review and editing, visualization, supervision, project administration, funding acquisition.

Conflicts of interest

There are no conflicts to declare.

Acknowledgements

Acknowledgment is made to the Donors of the American Chemical Society Petroleum Research Fund for support of this research (grant number 62578-DNI5). A. M. M. is grateful for start-up funds from the University of Rochester.

Notes and references

1 T. Taseska, W. Yu, M. K. Wilsey, C. P. Cox, Z. Meng, S. S. Ngarnim and A. M. Müller, *Top. Catal.*, 2023, **66**, 338–374.
2 M. Busch, N. B. Halck, U. I. Kramm, S. Siahrostami, P. Krtil and J. Rossmeisl, *Nano Energy*, 2016, **29**, 126–135.
3 S. Siahrostami, G.-L. Li, V. Viswanathan and J. K. Nørskov, *J. Phys. Chem. Lett.*, 2017, **8**, 1157–1160.
4 H. Lv, J. Song, Y. V. Geletii, J. W. Vickers, J. M. Sumliner, D. G. Musaev, P. Kögerler, P. F. Zhuk, J. Bacsa, G. Zhu and C. L. Hill, *J. Am. Chem. Soc.*, 2014, **136**, 9268–9271.
5 Y. V. Geletii, B. Botar, P. Kogerler, D. A. Hillesheim, D. G. Musaev and C. L. Hill, *Angew. Chem.*, 2008, **120**, 3960.
6 A. Kulkarni, S. Siahrostami, A. Patel and J. K. Nørskov, *Chem. Rev.*, 2018, **118**, 2302–2312.
7 X. Yang, Y. Zeng, W. Alnoush, Y. Hou, D. Higgins and G. Wu, *Adv. Mater.*, 2022, **34**, 2107954.
8 D. Higgins, P. Zamani, A. Yu and Z. Chen, *Energy Environ. Sci.*, 2016, **9**, 357–390.
9 B. Kumar, M. Llorente, J. Froehlich, T. Dang, A. Sathrum and C. P. Kubiak, *Annu. Rev. Phys. Chem.*, 2012, **63**, 541–569.
10 C. W. Machan, M. D. Sampson, S. A. Chabolla, T. Dang and C. P. Kubiak, *Organometallics*, 2014, **33**, 4550–4559.
11 D. K. Dogutan and D. G. Nocera, *Acc. Chem. Res.*, 2019, **52**, 3143–3148.
12 T. Faunce, S. Styring, M. R. Wasielewski, G. W. Brudvig, A. W. Rutherford, J. Messinger, A. F. Lee, C. L. Hill, H. Degroot and M. Fontecave, *Energy Environ. Sci.*, 2013, **6**, 1074–1076.
13 W. Li, J. Wu, D. C. Higgins, J.-Y. Choi and Z. Chen, *ACS Catal.*, 2012, **2**, 2761–2768.
14 E. Nikolla, J. Schwank and S. Linic, *J. Am. Chem. Soc.*, 2009, **131**, 2747–2754.
15 X.-K. Gu, J. S. Carneiro, S. Samira, A. Das, N. M. Ariyasingha and E. Nikolla, *J. Am. Chem. Soc.*, 2018, **140**, 8128–8137.
16 M. Karamad, R. Magar, Y. Shi, S. Siahrostami, I. D. Gates and A. B. Farimani, *Phys. Rev. Mater.*, 2020, **4**, 093801.
17 S. Siahrostami, C. Tsai, M. Karamad, R. Koitz, M. García-Melchor, M. Bajdich, A. Vojvodic, F. Abild-Pedersen, J. K. Nørskov and F. Studt, *Catal. Lett.*, 2016, **146**, 1917–1921.
18 S. Rondinini, C. Locatelli, A. Minguzzi and A. Vertova, *Electrochemical water and wastewater treatment*, Elsevier, 2018, pp. 3–28.
19 E. T. Martin, C. M. McGuire, M. S. Mubarak and D. G. Peters, *Chem. Rev.*, 2016, **116**, 15198–15234.
20 S. Manzetti, E. R. van der Spoel and D. van der Spoel, *Chem. Res. Toxicol.*, 2014, **27**, 713–737.
21 W. Guo, B. Pan, S. Sakkiah, G. Yavas, W. Ge, W. Zou, W. Tong and H. Hong, *Int. J. Environ. Res. Public Health*, 2019, **16**, 4361.
22 B. Yuan, K. Vorkamp, A. M. Roos, S. Faxneld, C. Sonne, S. E. Garbus, Y. Lind, I. Eulaers, P. Hellström and R. Dietz, *Environ. Sci. Technol.*, 2019, **53**, 3526–3537.
23 A. Covaci, S. Harrad, M. A.-E. Abdallah, N. Ali, R. J. Law, D. Herzke and C. A. de Wit, *Environ. Int.*, 2011, **37**, 532–556.
24 D. C. Muir and P. H. Howard, *Environ. Sci. Technol.*, 2006, **40**, 7157–7166.
25 Z. Chen, Y. Liu, W. Wei and B.-J. Ni, *Environ. Sci. Nano*, 2019, **6**, 2332–2366.
26 C. K. da Silva-Rackov, W. A. Lawal, P. A. Nfodzo, M. M. Vianna, C. A. do Nascimento and H. Choi, *Appl. Catal. B: Environ.*, 2016, **192**, 253–259.
27 J. N. Meegoda, B. Bezerra de Souza, M. M. Casarini and J. A. Kewalramani, *Int. J. Environ. Res. Public Health*, 2022, **19**, 16397.
28 P. Adriaens, C. Gruden and M. McCormick, *Treatise Geochem.*, 2003, **9**, 612.
29 G. W. Gribble, *J. Chem. Educ.*, 2004, **81**, 1441.
30 P. R. S. Kodavanti and B. G. Loganathan, *The international encyclopedia of public health*, ed. S. R. Quah, W. C. Cockerham, 2017, vol. 5, pp. 359–366.
31 M. Dorner, S. Lokesh, Y. Yang and S. Behrens, *Sci. Total Environ.*, 2022, 158381.
32 L. Melymuk, J. Blumenthal, O. E. Sáňka, A. Shu-Yin, V. Singla, K. I. Šebková, K. Pullen Fedinick and M. L. Diamond, *Environ. Sci. Technol.*, 2022, **56**, 9029–9040.
33 M. Sharkey, S. Harrad, M. A.-E. Abdallah, D. S. Drage and H. Berresheim, *Environ. Int.*, 2020, **144**, 106041.
34 U. EPA, *United States Environmental Protection Agency*, Washington, DC, 2010.
35 U. Unep, *United Nations environment programme: Stockholm convention on persistent organic pollutants*, Geneva, 2009, p. 112.
36 M. G. Alalm and D. C. Boffito, *Chem. Eng. J.*, 2022, 138352.
37 F. Liu, X. Guan and F. Xiao, *J. Hazard. Mater.*, 2022, 129580.
38 P. Höhener, D. Werner, C. Balsiger and G. Pasteris, *Worldwide occurrence and fate of chlorofluorocarbons in groundwater*, 2003.
39 L. M. Western, M. K. Vollmer, P. B. Krummel, K. E. Adcock, P. J. Fraser, C. M. Harth, R. L. Langenfelds, S. A. Montzka, J. Mühle and S. O'Doherty, *Nat. Geosci.*, 2023, 1–5.
40 L. Yin, Z. Shen, J. Niu, J. Chen and Y. Duan, *Environ. Sci. Technol.*, 2010, **44**, 9117–9122.
41 E. O. Igbinosa, E. E. Odjadjare, V. N. Chigor, I. H. Igbinosa, A. O. Emoghene, F. O. Ekhaise, N. O. Igiehon and O. G. Idemudia, *Sci. World J.*, 2013, **2013**, 60215.
42 P. H. Howard, *Handbook of environmental degradation rates*, CRC Press, 1991.
43 A. J. Jamieson, T. Malkocs, S. B. Piertney, T. Fujii and Z. Zhang, *Nat. Ecol. Evol.*, 2017, **1**, 1–4.
44 W. M. Caudle, T. S. Guillot, C. R. Lazo and G. W. Miller, *Neurotoxicology*, 2012, **33**, 178–188.
45 S. Ullah, M. W. Javed, M. Shafique and S. F. Khan, *J. Himal. Earth Sci.*, 2014, **47**, 163–174.
46 M. V. Russo, I. Notardonato, A. Rosada, G. Ianiri and P. Avino, *Int. J. Environ. Res. Public Health*, 2021, **18**, 1628.
47 S.-L. Badea, E.-I. Geana, V.-C. Niculescu and R.-E. Ionete, *Sci. Total Environ.*, 2020, **722**, 137914.
48 G. R. Chaudhry and S. Chapalamadugu, *Microbiol. Rev.*, 1991, **55**, 59–79.
49 H. G. Ni, H. Zeng, S. Tao and E. Y. Zeng, *Environ. Toxicol. Chem.*, 2010, **29**, 1237–1247.
50 S. S. Zumdahl and S. A. Zumdahl, *Chemistry*, Cengage Learning, 2013.
51 Y. Guo, Y. Li and Z. Wang, *Water Res.*, 2023, 119810.
52 C. Choi, X. Wang, S. Kwon, J. L. Hart, C. L. Rooney, N. J. Harmon, Q. P. Sam, J. J. Cha, W. A. Goddard III and M. Elimelech, *Nat. Nanotechnol.*, 2023, **18**, 160–167.
53 C. Wolf, C. Lambright, P. Mann, M. Price, R. L. Cooper, J. Ostby and L. E. Gray Jr, *Toxicol. Ind. Health*, 1999, **15**, 94–118.
54 G. Buck Louis, J. Weiner, B. Whitcomb, R. Sperrazza, E. Schisterman, D. Lobdell, K. Crickard, H. Greizerstein and P. Kostyniak, *Hum. Reprod.*, 2005, **20**, 279–285.
55 H. I. Zeliger, *Rev. Environ. Health*, 2013, **28**, 9–20.
56 S. L. Schantz, J. J. Widholm and D. C. Rice, *Environ. Health Perspect.*, 2003, **111**, 357–576.
57 V. J. Cogliano, *Environ. Health Perspect.*, 1998, **106**, 317–323.
58 J. A. Goldstein, P. Hickman, H. Bergman, J. D. Mckinney and M. P. Walker, *Chem.-Biol. Interact.*, 1977, **17**, 69–87.
59 B. McHugh, R. Poole, J. Corcoran, P. Anninou, B. Boyle, E. Joyce, M. B. Foley and E. McGovern, *Chemosphere*, 2010, **79**, 305–313.
60 Material and Chemicals – Brominated Flame Retardant (BFR) Market, **https://www.reportsanddata.com/report-detail/brominated-flame-retardant-market**, accessed June 20, 2023.

61 C. A. De Wit, *Chemosphere*, 2002, **46**, 583–624.
62 J. Chevrier, K. G. Harley, A. Bradman, M. Gharbi, A. Sjödin and B. Eskenazi, *Environ. Health Perspect.*, 2010, **118**, 1444–1449.
63 T. Okazoe, *Proc. Jpn. Acad., Ser. B*, 2009, **85**, 276–289.
64 S. M. S. Hussain, A. A. Adewunmi, A. Mahboob, M. Murtaza, X. Zhou and M. S. Kamal, *Adv. Colloid Interface Sci.*, 2022, 102634.
65 Z. Yue, H. Dunya, S. Aryal, C. U. Segre and B. Mandal, *J. Power Sources*, 2018, **401**, 271–277.
66 D. Schrenk, M. Bignami, L. Bodin, J. K. Chipman, J. del Mazo, B. Grasl-Kraupp, C. Hogstrand, L. Hoogenboom and J. C. Leblanc, *EFSA J.*, 2020, **18**, e06223.
67 R. Lohmann, I. T. Cousins, J. C. DeWitt, J. Gluge, G. Goldenman, D. Herzke, A. B. Lindstrom, M. F. Miller, C. A. Ng and S. Patton, *Environ. Sci. Technol.*, 2020, **54**, 12820–12828.
68 E. Gagliano, M. Sgroi, P. P. Falciglia, F. G. Vagliasindi and P. Roccaro, *Water Res.*, 2020, **171**, 115381.
69 L. N. Plummer and E. Busenberg, *Environmental tracers in subsurface hydrology*, 2000, pp. 441–478.
70 M. K. Vollmer, J. Mühle, S. Henne, D. Young, M. Rigby, B. Mitrevski, S. Park, C. R. Lunder, T. S. Rhee and C. M. Harth, *Proc. Natl. Acad. Sci. U. S. A.*, 2021, **118**, e2010914118.
71 M. Wernke, *Encyclopedia of Toxicology*, 3rd edn, 2014, pp. 664–666.
72 M. McFarland, *Proc. Natl. Acad. Sci. U. S. A.*, 1992, **89**, 807–811.
73 W.-T. Tsai, *Chemosphere*, 2005, **61**, 1539–1547.
74 E. A. Ural, *Process Saf. Prog.*, 2003, **22**, 65–73.
75 Forever Chemicals and the Advancement of Filtration Standards, **https://www.nsf.org/knowledge-library/forever-chemicals-advancement-filtration-standards**, accessed June 14, 2023.
76 J. Glüge, M. Scheringer, I. T. Cousins, J. C. DeWitt, G. Goldenman, D. Herzke, R. Lohmann, C. A. Ng, X. Trier and Z. Wang, *Environ. Sci.: Process Impacts*, 2020, **22**, 2345–2373.
77 J. W. Washington and T. M. Jenkins, *Environ. Sci. Technol.*, 2015, **49**, 14129–14135.
78 J. Garnett, C. Halsall, H. Winton, H. Joerss, R. Mulvaney, R. Ebinghaus, M. Frey, A. Jones, A. Leeson and P. Wynn, *Environ. Sci. Technol.*, 2022, **56**, 11246–11255.
79 M. E. Andersen, B. Hagenbuch, U. Apte, J. C. Corton, T. Fletcher, C. Lau, W. L. Roth, B. Staels, G. L. Vega and H. J. Clewell, *Toxicology*, 2021, **459**, 152845.
80 S. Kurwadkar, J. Dane, S. R. Kanel, M. N. Nadagouda, R. W. Cawdrey, B. Ambade, G. C. Struckhoff and R. Wilkin, *Sci. Total Environ.*, 2022, **809**, 151003.
81 H. N. Phong Vo, H. H. Ngo, W. Guo, T. M. Hong Nguyen, J. Li, H. Liang, L. Deng, Z. Chen and T. A. Hang Nguyen, *J. Water Process. Eng.*, 2020, **36**, 101393.
82 S. Sharma, N. P. Shetti, S. Basu, M. N. Nadagouda and T. M. Aminabhavi, *Chem. Eng. J.*, 2022, **430**, 132895.
83 D. Benford, J. De Boer, A. Carere, A. Di Domenico, N. Johansson, D. Schrenk, G. Schoeters, P. De Voogt and E. Dellatte, *EFSA J.*, 2008, **653**, 1–131.
84 K. Steenland and A. Winquist, *Environ. Res.*, 2021, **194**, 110690.
85 E. M. Sunderland, X. C. Hu, C. Dassuncao, A. K. Tokranov, C. C. Wagner and J. G. Allen, *J. Expo. Sci. Environ. Epidemiol.*, 2019, **29**, 131–147.
86 M. Averina, J. Brox, S. Huber, A.-S. Furberg and M. Sørensen, *Environ. Res.*, 2019, **169**, 114–121.
87 N. Ding, C. A. Karvonen-Gutierrez, B. Mukherjee, A. M. Calafat, S. D. Harlow and S. K. Park, *Hypertension*, 2022, **79**, 1876–1886.
88 P. Grandjean, E. W. Andersen, E. Budtz-Jørgensen, F. Nielsen, K. Mølbak, P. Weihe and C. Heilmann, *JAMA*, 2012, **307**, 391–397.
89 B. M. Sharma, G. K. Bharat, S. Tayal, T. Larssen, J. Bečanová, P. Karásková, P. G. Whitehead, M. N. Futter, D. Butterfield and L. Nizzetto, *Environ. Pollut.*, 2016, **208**, 704–713.
90 D. Leonello, M. A. Fendrich, F. Parrino, N. Patel, M. Orlandi and A. Miotello, *Appl. Sci.*, 2021, **11**, 8458.
91 Z. Zeng, B. Song, R. Xiao, G. Zeng, J. Gong, M. Chen, P. Xu, P. Zhang, M. Shen and H. Yi, *Environ. Int.*, 2019, **126**, 598–610.
92 J. Zodrow, U. Vedagiri, T. Sorell, L. McIntosh, E. Larson, L. Hall, M. Dourson, L. Dell, D. Cox and K. Barfoot, *Remediation*, 2022, **32**, 29–44.
93 National Primary Drinking Water Regulations, **https://www.epa.gov/ground-water-and-drinking-water/national-primary-drinking-water-regulations#Organic**, accessed June 20, 2023.
94 J. A. Roberson, *Forever Chemicals*, CRC Press, 2021, pp. 87–97.
95 M. Gmurek, M. Olak-Kucharczyk and S. Ledakowicz, *Chem. Eng. J.*, 2017, **310**, 437–456.
96 S. Garcia-Segura, J. D. Ocon and M. N. Chong, *Process Saf. Environ. Prot.*, 2018, **113**, 48–67.
97 E. Hepburn, C. Madden, D. Szabo, T. L. Coggan, B. Clarke and M. Currell, *Environ. Pollut.*, 2019, **248**, 101–113.
98 G. M. Sinclair, S. M. Long and O. A. Jones, *Chemosphere*, 2020, **258**, 127340.
99 E. Kostyal, M. Borsanyi, L. Rigottier-Gois and M. S. Salkinoja-Salonen, *Appl. Microbiol. Biotechnol.*, 1998, **50**, 612–622.
100 A. J. Toth, E. Haáz, T. Nagy, A. J. Tarjani, D. Fozer, A. Andre, N. Valentinyi and P. Mizsey, *Desalination Water Treat*, 2018, **120**, 2–29.
101 R. Xu, Y. Xie, J. Tian and L. Chen, *J. Clean. Prod.*, 2021, **283**, 124645.
102 M. N. Rashed, *Adsorption technique for the removal of organic pollutants from water and wastewater*, 2013.
103 C. Xu, R. Liu, W. Zheng, L. Lin and L. Chen, *Water*, 2021, **13**, 1543.
104 S. Sharma and A. Bhattacharya, *Appl. Water Sci.*, 2017, **7**, 1043–1067.
105 K. Urano, E. Yamamoto, M. Tonegawa and K. Fujie, *Water Res.*, 1991, **25**, 1459–1464.
106 X. Li, H. Liu, X. Jia, G. Li, T. An and Y. Gao, *Sci. Total Environ.*, 2018, **621**, 1533–1541.
107 G. Liu, H. Sheng, Y. Fu, Y. Song, M. Redmile-Gordon, Y. Qiao, C. Gu, L. Xiang and F. Wang, *Chemosphere*, 2019, **214**, 176–183.
108 Y. Zhu, X. Li, L. Wang, N. Hui, J. Ma and F. Chen, *Water Air Soil Pollut.*, 2021, **232**, 494.
109 C. Rodriguez, A. Cook, B. Devine, P. Van Buynder, R. Lugg, K. Linge and P. Weinstein, *Int. J. Environ. Res. Public Health*, 2008, **5**, 356–367.
110 C. A. Martínez-Huitle, M. A. Rodrigo, I. Sirés and O. Scialdone, *Chem. Rev.*, 2015, **115**, 13362–13407.
111 A. Urtiaga, *Curr. Opin. Electrochem.*, 2021, **27**, 100691.
112 S. C. E. Leung, P. Shukla, D. Chen, E. Eftekhari, H. An, F. Zare, N. Ghasemi, D. Zhang, N.-T. Nguyen and Q. Li, *Sci. Total Environ.*, 2022, 153669.
113 S. Khan, M. Sayed, M. Sohail, L. A. Shah and M. A. Raja, *Advances in water purification techniques*, 2019, pp. 135–164.
114 A. Yazdanbakhsh, A. Eslami, G. Moussavi, M. Rafiee and A. Sheikhmohammadi, *Chemosphere*, 2018, **191**, 156–165.
115 C. Comninellis, A. Kapalka, S. Malato, S. A. Parsons, I. Poulios and D. Mantzavinos, *J. Chem. Technol. Biotechnol.*, 2008, **83**, 769–776.
116 C. Cao, *Sci. China, Ser. B: Chem.*, 2009, **52**, 943–951.
117 A. S. Menon, G. P. Wood, D. Moran and L. Radom, *J. Phys. Chem. A*, 2007, **111**, 13638–13644.
118 X.-M. Zhang, *J. Chem. Soc., Perkin Trans. 2*, 1993, 2275–2279.
119 K. Daasbjerg, *J. Chem. Soc., Perkin Trans. 2*, 1994, 1275–1277.
120 F. Li, J. Duan, S. Tian, H. Ji, Y. Zhu, Z. Wei and D. Zhao, *Chem. Eng. J.*, 2020, **380**, 122506.
121 X. Xiong, Y. Shang, L. Bai, S. Luo, T. W. Seviour, Z. Guo, L. D. Ottosen and Z. Wei, *Water Res.*, 2023, **235**, 119829.
122 Y. Su, U. Rao, C. M. Khor, M. G. Jensen, L. M. Teesch, B. M. Wong, D. M. Cwiertny and D. Jassby, *ACS Appl. Mater. Interfaces*, 2019, **11**, 33913–33922.
123 J. Liu, D. J. Van Hoomissen, T. Liu, A. Maizel, X. Huo, S. R. Fernández, C. Ren, X. Xiao, Y. Fang and C. E. Schaefer, *Environ. Sci. Technol. Lett.*, 2018, **5**, 289–294.
124 G. Cavallo, P. Metrangolo, R. Milani, T. Pilati, A. Priimagi, G. Resnati and G. Terraneo, *Chem. Rev.*, 2016, **116**, 2478–2601.
125 H. N. Lynch, R. L. Prueitt and J. E. Goodman, *Regul. Toxicol. Pharmacol.*, 2018, **97**, 189–196.
126 Drinking Water Notification Levels, **https://www.waterboards.ca.gov/drinking_water/certlic/drinkingwater/NotificationLevels.html**, accessed August 8, 2023.
127 EPA, Drinking Water Health Advisories (HAs), **https://www.epa.gov/sdwa/drinking-water-health-advisories-has**, accessed August 26, 2023.
128 Amendment of Subpart 5-1 of Title 10 NYCRR (Maximum Contaminant Levels (MCLs)), **https://regs.health.ny.gov/regulations/proposed-rule-making**, accessed August 8, 2023.
129 US EPA, Fifth Unregulated Contaminant Monitoring Rule, **https://www.epa.gov/dwucmr/fifth-unregulated-contaminant-monitoring-rule**, accessed August 8, 2023.
130 PFAS: Per- and Polyfluoroalkyl Substances, **https://www.waterboards.ca.gov/drinking_water/certlic/drinkingwater/pfas.html**, accessed August 8, 2023.

131 California Drinking Water Standards, https://www.gswater.com/sites/main/files/file-attachments/california-drinking-water-standards-rev-21218.pdf?1658793570, accessed August 27, 2023.
132 New Jersey Department of Health and Senior Services, Hazardous Substance Fact Sheet: Trichlorofluoro-Methane https://nj.gov/health/eoh/rtkweb/documents/fs/1891.pdf, accessed August 8, 2023.
133 California Water Boards, Drinking Water Notification Levels and Response Levels: An Overview, https://www.waterboards.ca.gov/drinking_water/certlic/drinkingwater/NotificationLevels.html, accessed August 8, 2023.
134 New Jersey Department of Health and Senior Services, Hazardous Substance Fact Sheet: Dichlorodifluoro-Methane, https://nj.gov/health/eoh/rtkweb/documents/fs/0649.pdf, accessed August 8, 2023.
135 Chlorotrifluoromethane, https://cameochemicals.noaa.gov/chemical/2934, accessed August 27, 2023.
136 New Jersey Department of Health and Senior Services, Hazardous Substance Fact Sheet: Chlorotrifluoro-Methane, https://www.nj.gov/health/eoh/rtkweb/documents/fs/0425.pdf, accessed August 8, 2023.
137 New Jersey Department of Health, Hazardous Substance Fact Sheet: Chlorodifluoromethane, https://nj.gov/health/eoh/rtkweb/documents/fs/0386.pdf, accessed August 8, 2023.
138 National Refrigerants, Inc., Safety Data Sheet: 1,Chloro-1,1difluoroethane, https://refrigerants.com/wp-content/uploads/2020/01/SDS-R142b.pdf, accessed August 8, 2023.
139 US OSHA, Occupational Chemical Database: 1,1-Dichloro-1-fluoroethane, https://www.osha.gov/chemicaldata/814, accessed August 8, 2023.
140 EPA, Consumer Factsheet on: Vinyl Chloride, https://archive.epa.gov/water/archive/web/pdf/archived-consumer-fact-sheet-on-vinyl-chloride.pdf, accessed August 27, 2023.
141 Vinyl Chloride and Drinking Water, https://www.health.state.mn.us/communities/environment/risk/docs/guidance/gw/vinylchlorideinfo.pdf, accessed August 27, 2023.
142 New Jersey Department of Health, Hazardous Substance Fact Sheet: Vinyl Chloride, https://nj.gov/health/eoh/rtkweb/documents/fs/2001.pdf, accessed August 8, 2023.
143 US EPA, Acute Exposure Guidelines Levels: 1,2-Dichloroethene, https://www.epa.gov/sites/default/files/2014-11/documents/1_2_dichloroethylene_final_volume_8.pdf, accessed August 8, 2023.
144 New Jersey Department of Health, Hazardous Substance Fact Sheet: Tetrachloroethylene, https://nj.gov/health/eoh/rtkweb/documents/fs/1810.pdf, accessed August 8, 2023.
145 New Jersey Department of Health, Hazardous Substance Fact Sheet: trichloroethylene, https://nj.gov/health/eoh/rtkweb/documents/fs/1890.pdf, accessed August 8, 2023.
146 Ambient Water Quality Criteria for 2-chlorophenol, https://www.epa.gov/sites/default/files/2018-12/documents/ambient-wqc-2chlorophenol.pdf accessed August 27, 2023.
147 Agilent, Safety Data Sheet: 2-Chlorophenol, https://www.agilent.com/cs/library/msds/RCP-001_NAEnglish.pdf, accessed August 8, 2023.
148 US EPA, Consumer Fact Sheet on: Dioxin (2,3,7,8-TCDD), https://archive.epa.gov/water/archive/web/pdf/archived-consumer-fact-sheet-on-dioxin.pdf, accessed August 8, 2023.
149 US OSHA, Permissible Exposure Limits – Annotated Tables, https://www.osha.gov/annotated-pels/table-z-1, accessed August 8, 2023.
150 Canadian Environmental Protection Act, 1999, https://www.ec.gc.ca/ese-ees/default.asp?lang=En&n=05DF7A37-1, accessed August 27, 2023.
151 Bluesign, Threshold Limit Values for Chemical Substances in Chemical Products, https://www.bluesign.com/downloads/bsbl/2023/bsbl_v50.pdf, accessed August 8, 2023.
152 US Department of Health and Human Services, NTP Nomination History and Review: 2,4,6-Tribromophenol, https://ntp.niehs.nih.gov/sites/default/files/ntp/htdocs/chem_background/exsumpdf/tribromophenol_508.pdf, accessed August 8, 2023.
153 Amending Regulation (EC) No. 850/2004 of the European Parliament and of the Council on Persistent Organic Pollutants as Regard Annex 1, https://eur-lex.europa.eu/legal-content/EN/TXT/PDF/?uri=CELEX:32016R0293&from=DE, accessed August 8, 2023.
154 Tetrabromobisphenol A, https://ntp.niehs.nih.gov/sites/default/files/ntp/htdocs/chem_background/exsumpdf/tetrabromobisphenola_508.pdf, accessed August 27, 2023.
155 US Department of Health and Human Services, Review of Toxicological Literature: Tetrabromobisphenol A, https://ntp.niehs.nih.gov/sites/default/files/ntp/htdocs/chem_background/exsumpdf/tetrabromobisphenola_508.pdf, accessed August 8, 2023.
156 Agricultural Operations Notifications and Reporting Requirement https://media.defense.gov/2021/Nov/19/2002896203/-1/-1/0/AGRICULTURAL-OPERATIONS-NOTIFICATIONS-AND-REPORTING-REQUIREMENT.PDF, accessed August 27, 2023.
157 S.-I. Sakai, K. Hayakawa, H. Takatsuki and I. Kawakami, *Environ. Sci. Technol.*, 2001, **35**, 3601–3607.
158 Q. Huang and C. Fang, *Sci. Total Environ.*, 2020, **739**, 139926.
159 Z. Zhang, J.-J. Chen, X.-J. Lyu, H. Yin and G.-P. Sheng, *Sci. Rep.*, 2014, **4**, 1–6.
160 N. R. Council, Waste incineration and public health, 2000.
161 L. Makarichi, W. Jutidamrongphan and K.-A. Techato, *Renewable Sustainable Energy Rev.*, 2018, **91**, 812–821.
162 A. G. Capodaglio, *Appl. Sci.*, 2020, **10**, 4549.
163 K.-I. Naicker, P. Kaweesa, M. O. Daramola and S. A. Iwarere, *Appl. Sci.*, 2023, **13**, 6243.
164 M. A. Malik, *Plasma Chem. Plasma Process.*, 2010, **30**, 21–31.
165 X. Hou, G. Zhan, X. Huang, N. Wang, Z. Ai and L. Zhang, *Chem. Eng. J.*, 2020, **382**, 122355.
166 D. C. Schmelling, D. L. Poster, M. Chaychian, P. Neta, J. Silverman and M. Al-Sheikhly, *Environ. Sci. Technol.*, 1998, **32**, 270–275.
167 R. M. Morrison, *An economic analysis of electron accelerators and cobalt-60 for irradiating food*, US Department of Agriculture, Economic Research Service, Rockville, MD, USA, 1989.
168 T. A. Saleh, M. Mustaqeem and M. Khaled, *Environ. Nanotechnol. Monit. Manag*, 2022, **17**, 100617.
169 H. Md Anawar and R. Chowdhury, *Sustainability*, 2020, **12**, 7017.
170 X. Bai, X. Zhu, H. Jiang, Z. Wang, C. He, L. Sheng and J. Zhuang, *Water*, 2020, **12**, 1054.
171 W.-x Zhang, C.-B. Wang and H.-L. Lien, *Catal. Today*, 1998, **40**, 387–395.
172 K.-C. Huang, G. E. Hoag, P. Chheda, B. A. Woody and G. M. Dobbs, *J. Hazard. Mater.*, 2001, **87**, 155–169.
173 Z. Ronen and A. Abeliovich, *Appl. Environ. Microbiol.*, 2000, **66**, 2372–2377.
174 J. Radjenovic and D. L. Sedlak, *Environ. Sci. Technol.*, 2015, **49**, 11292–11302.
175 H. Wang and J. Wang, *Appl. Catal. B: Environ.*, 2007, **77**, 58–65.
176 C. A. Martinez-Huitle and S. Ferro, *Chem. Soc. Rev.*, 2006, **35**, 1324–1340.
177 J. Qiao and Y. Xiong, *J. Water Process Eng.*, 2021, **44**, 102308.
178 B. Yang, H. Li, Z. Zhang, K. Xiao, M. Yang, F. Zhang, M. Wang, X. Guo, Q. Li and W. Fu, *Chem. Eng. J.*, 2022, **427**, 131719.
179 L. Yang, C. Huang, Z. Yin, J. Meng, M. Guo, L. Feng, Y. Liu, L. Zhang and Z. Du, *Chemosphere*, 2021, **264**, 128515.
180 M. P. Rayaroth, C. T. Aravindakumar, N. S. Shah and G. Boczkaj, *Chem. Eng. J.*, 2022, **430**, 133002.
181 H. Feng, X. Liao, R. Yang, S. Chen, Z. Zhang, J. Tong, J. Liu and X. Wang, *Water Res.*, 2023, **230**, 119531.
182 E. Domingues, E. Fernandes, J. Gomes and R. C. Martins, *Sci. Total Environ.*, 2021, **776**, 145958.
183 M. Lei, N. Wang, S. Guo, L. Zhu, Y. Ding and H. Tang, *Chem. Eng. J.*, 2018, **345**, 586–593.
184 Y. Wei, Y. Gong, X. Zhao, Y. Wang, R. Duan, C. Chen, W. Song and J. Zhao, *Environ. Sci. Nano*, 2019, **6**, 1585–1593.
185 R. A. Torres-Palma and E. A. Serna-Galvis, *Advanced oxidation processes for waste water treatment*, Elsevier, 2018, pp. 177–213.
186 R. Xiao, Z. Wei, D. Chen and L. K. Weavers, *Environ. Sci. Technol.*, 2014, **48**, 9675–9683.
187 J. Blotevogel, S. M. Thagard and S. Mahendra, *Curr. Opin. Chem. Eng.*, 2023, **41**, 100944.
188 A. Asghar, A. A. A. Raman and W. M. A. W. Daud, *J. Clean. Prod.*, 2015, **87**, 826–838.
189 J. González-García, V. Sáez, I. Tudela, M. I. Díez-Garcia, M. Deseada Esclapez and O. Louisnard, *Water*, 2010, **2**, 28–74.
190 M. H. Lim, S. H. Kim, Y. U. Kim and J. Khim, *Ultrason. Sonochem.*, 2007, **14**, 93–98.
191 D. Panda, V. Sethu and S. Manickam, *Environ. Technol. Innovation*, 2020, **17**, 100605.
192 D. Panda and S. Manickam, *Sep. Purif. Technol.*, 2019, **209**, 914–920.

193 H. Wang, C. Zhang, X. Zhang, S. Wang, Z. Xia, G. Zeng, J. Ding and N. Ren, *Chem. Eng. J.*, 2022, **429**, 132445.
194 S. Khammar, N. Bahramifar and H. Younesi, *J. Hazard. Mater.*, 2020, **394**, 122422.
195 Q. Zheng, Z. Liu, L. Yang, J. Lu, C. Qiu, X. Guan and K. Yan, *Chem. Eng. J.*, 2020, **387**, 124005.
196 A. T. Dao, S. J. Loenen, K. Swart, H. T. Dang, A. Brouwer and T. E. de Boer, *Chemosphere*, 2021, **263**, 128280.
197 N. B. Varzaghani, S. Shokrollahzadeh and A. Farazmand, *J. Environ. Chem. Eng.*, 2021, **9**, 105098.
198 F. Escalona-Durán, M. Muñoz-Morales, F. Souza, C. Sáez, P. Cañizares, C. Martínez-Huitle and M. Rodrigo, *Chemosphere*, 2021, **279**, 130525.
199 N. D. Mohamad, Z. M. Zaki and A. Amir, *Chem. Eng. J.*, 2020, **393**, 124760.
200 Y. Lyu, S. Lyu, P. Tang, W. Jiang, Y. Sun, M. Li and Q. Sui, *Chemosphere*, 2020, **257**, 127223.
201 Y. Sun, M. Danish, M. Ali, A. Shan, M. Li, Y. Lyu, Z. Qiu, Q. Sui, X. Zang and S. Lyu, *Chem. Eng. J.*, 2020, **394**, 124830.
202 M. Ali, M. Danish, M. Tariq, A. Ahmad, K. S. Ayub and S. Lyu, *Chem. Eng. J.*, 2020, **399**, 125754.
203 F. Li, D. Deng, L. Zeng, S. Abrams and M. Li, *Sci. Total Environ.*, 2021, **774**, 145118.
204 A. Venkateshaiah, D. Silvestri, S. Wacławek, R. K. Ramakrishnan, K. Krawczyk, P. Saravanan, M. Pawlyta, V. V. Padil, M. Černík and D. D. Dionysiou, *Environ. Sci. Water Res. Technol.*, 2022, **8**, 162–172.
205 M. Dutschke, T. Schnabel, F. Schütz and C. Springer, *J. Environ. Manage.*, 2022, **304**, 114236.
206 Y.-C. Chang, M. V. Reddy and D. Choi, *Green Chem.*, 2021, **23**, 2729–2737.
207 Z. Chen, L. Wang, H. Xu and Q. Wen, *Chem. Eng. J.*, 2020, **389**, 124345.
208 Q. Wang, T. Wang, G. Qu, Y. Zhang, Q. Sun, X. Guo and H. Jia, *Sep. Purif. Technol.*, 2020, **240**, 116615.
209 C. Hou, W. Chen, L. Fu, S. Zhang, C. Liang and Y. Wang, *Carbohydr. Polym.*, 2020, **247**, 116731.
210 C. Fang, X. Lou, Y. Tang, L. Tian, Y. Cai, D. Xiao, Y. Guo and J. Liu, *J. Environ. Chem. Eng.*, 2020, **8**, 103998.
211 L. Fu, F. Lide, Y. Ding, C. Wang, J. Jiang and J. Huang, *Sep. Purif. Technol.*, 2022, **285**, 120282.
212 T.-H. Chang, R. Wang, Y.-H. Peng, T.-H. Chou, Y.-J. Li and Y.-H. Shih, *Chemosphere*, 2020, **246**, 125621.
213 T. Li, Y. Lu, L. Liu, Y. He, J. Huang and X. Peng, *J. Hazard. Mater.*, 2023, 131739.
214 Y. Jiang, S. Yang, J. Liu, T. Ren, Y. Zhang and X. Sun, *Chemosphere*, 2020, **244**, 125536.
215 Y. Jiang, S. Yang, M. Wang, Y. Xue, J. Liu, Y. Li and D. Zhao, *Chemosphere*, 2021, **279**, 130520.
216 L. Wei, B. Zhou, K. Xiao, B. Yang, G. Yu, J. Li, C. Zhu, J. Zhang and H. Duan, *J. Hazard. Mater.*, 2020, **385**, 121551.
217 J. Liang, H. Liu, M. Zou, X. Tao, J. Zhou, Z. Dang and G. Lu, *Chemosphere*, 2023, **325**, 138396.
218 K. Huang, H. Liu, J. He, Y. He, X. Tao, H. Yin, Z. Dang and G. Lu, *J. Environ. Chem. Eng.*, 2021, **9**, 105077.
219 X. Xu, M. Liu, Y. Zhang and Y. Zhang, *S. Afr. J. Bot.*, 2023, **153**, 94–101.
220 X. Zhang, M. Feng, F. Liu, L. Qin, R. Qu, D. Li and Z. Wang, *Environ. Sci. Pollut. Res.*, 2014, **21**, 1924–1935.
221 Z. Wei, J. Xi, S. Gao, X. You, N. Li, Y. Cao, L. Wang, Y. Luan and X. Dong, *Sci. Rep.*, 2018, **8**, 5423.
222 T. Pan, Y. Wang, X. Yang, X.-F. Huang and R.-L. Qiu, *Chem. Eng. J.*, 2020, **384**, 123248.
223 Z. Guo, H. Yin, X. Wei, M. Zhu, G. Lu and Z. Dang, *J. Hazard. Mater.*, 2021, **415**, 125698.
224 J. Zhu, Y. Chen, Y. Gu, H. Ma, M. Hu, X. Gao and T. Liu, *J. Hazard. Mater.*, 2022, **422**, 126953.
225 B. Trang, Y. Li, X.-S. Xue, M. Ateia, K. Houk and W. R. Dichtel, *Science*, 2022, **377**, 839–845.
226 J. Niu, H. Lin, J. Xu, H. Wu and Y. Li, *Environ. Sci. Technol.*, 2012, **46**, 10191–10198.
227 H. Lin, J. Niu, S. Liang, C. Wang, Y. Wang, F. Jin, Q. Luo and Q. Huang, *Chem. Eng. J.*, 2018, **354**, 1058–1067.
228 S. Verma, B. Mezgebe, E. Sahle-Demessie and M. N. Nadagouda, *Chemosphere*, 2021, **280**, 130660.
229 I. K. A. Electrochemistry Kit: Boron Doped Diamond, **https://www.ika.com/en/Products-Lab-Eq/Electrochemistry-Kit-csp-516/Boron-doped-diamond,-Set-of-2-cpdt-40002856/**, accessed July 7, 2022.
230 N. N. Mahamuni and Y. G. Adewuyi, *Ultrason. Sonochem.*, 2010, **17**, 990–1003.
231 A. Blumberga, D. Blumberga, J. Pubule and F. Romagnoli, *Energy Procedia*, 2015, **72**, 170–174.
232 D. Panepinto, S. Fiore, G. Genon and M. Acri, *J. Clean. Prod.*, 2016, **137**, 1323–1329.
233 A. Guerrini, G. Romano and A. Indipendenza, *Sustainability*, 2017, **9**, 1126.
234 C. E. Schaefer, C. Andaya, A. Burant, C. W. Condee, A. Urtiaga, T. J. Strathmann and C. P. Higgins, *Chem. Eng. J.*, 2017, **317**, 424–432.
235 T. X. H. Le, H. Haflich, A. D. Shah and B. P. Chaplin, *Environ. Sci. Technol. Lett.*, 2019, **6**, 504–510.
236 X. Pang, J. T. Davis, A. D. Harvey and D. V. Esposito, *Energy Environ. Sci.*, 2020, **13**, 3663–3678.
237 D. Palma, C. Richard and M. Minella, *Chem. Eng. J. Adv.*, 2022, 100253.
238 A. Kimura, M. Taguchi, Y. Ohtani, Y. Shimada, H. Hiratsuka and T. Kojima, *Radiat. Phys. Chem.*, 2007, **76**, 699–706.
239 I. B. Rivas-Ortiz, G. Cruz-González, A. M. Lastre-Acosta, M. Manduca-Artiles, M. Rapado-Paneque, A. Chávez-Ardanza, A. C. S. C. Teixeira and U. J. Jáuregui-Haza, *J. Radioanal. Nucl. Chem.*, 2017, **314**, 2597–2607.
240 L. Barillas, presented in part at the Journal of Physics: Conference Series, 2015.
241 J.-C. Lin, C.-Y. Hu and S.-L. Lo, *Ultrason. Sonochem.*, 2016, **28**, 130–135.
242 C. Liu, K. Shih and F. Wang, *Sep. Purif. Technol.*, 2012, **87**, 95–100.
243 Y.-C. Lee, S.-L. Lo, J. Kuo and Y.-L. Lin, *Chem. Eng. J.*, 2012, **198**, 27–32.
244 M. J. Krause, E. Thoma, E. Sahle-Damesessie, B. Crone, A. Whitehill, E. Shields and B. Gullett, *J. Environ. Eng.*, 2022, **148**, 05021006.
245 J. Yang, S. Wang, Y. Li, Y. Zhang and D. Xu, *J. Environ. Manage.*, 2019, **233**, 131–140.
246 V. Vadillo, J. Sánchez-Oneto, J. R. Portela and E. J. M. de la Ossa, *Advanced Oxidation Processes for Waste Water Treatment*, Elsevier, 2018, pp. 333–358.
247 Q. Zhuo, S. Deng, B. Yang, J. Huang and G. Yu, *Environ. Sci. Technol.*, 2011, **45**, 2973–2979.
248 H. Lin, J. Niu, S. Ding and L. Zhang, *Water Res.*, 2012, **46**, 2281–2289.
249 H. Zhao, J. Gao, G. Zhao, J. Fan, Y. Wang and Y. Wang, *Appl. Catal.*, 2013, **136–137**, 278–286.
250 B. Yang, C. Jiang, G. Yu, Q. Zhuo, S. Deng, J. Wu and H. Zhang, *J. Hazard. Mater.*, 2015, **299**, 417–424.
251 Q. Zhuo, M. Luo, Q. Guo, G. Yu, S. Deng, Z. Xu, B. Yang and X. Liang, *Electrochim. Acta*, 2016, **213**, 358–367.
252 Z. Xu, Y. Yu, H. Liu and J. Niu, *Sci. Total Environ.*, 2017, **579**, 1600–1607.
253 Q. Zhuo, Q. Xiang, H. Yi, Z. Zhang, B. Yang, K. Cui, X. Bing, Z. Xu, X. Liang, Q. Guo and R. Yang, *J. Electroanal. Chem.*, 2017, **801**, 235–243.
254 H. Lin, J. Niu, S. Liang, C. Wang, Y. Wang, F. Jin, Q. Luo and Q. Huang, *Chem. Eng. J.*, 2018, **354**, 1058–1067.
255 S. Sharma, N. P. Shetti, S. Basu, M. N. Nadagouda and T. M. Aminabhavi, *Chem. Eng. J.*, 2022, **430**, 132895.
256 K. E. Carter and J. Farrell, *Environ. Sci. Technol.*, 2008, **42**, 6111–6115.
257 J. N. Uwayezu, I. Carabante, T. Lejon, P. van Hees, P. Karlsson, P. Hollman and J. Kumpiene, *J. Environ. Manage.*, 2021, **290**, 112573.
258 E. Amores, J. Rodriguez and C. Carreras, *Int. J. Hydrogen Energy*, 2014, **39**, 13063–13078.
259 F. Gaied, B. Louhichi, M. Bali and M. R. Jeday, *Songklanakarin J. Sci. Technol.*, 2019, **41**, 1084–1092.
260 U. Rao, Y. Su, C. M. Khor, B. Jung, S. Ma, D. M. Cwiertny, B. M. Wong and D. Jassby, *Environ. Sci. Technol.*, 2020, **54**, 10668–10677.
261 S. Huang, M. Sima, Y. Long, C. Messenger and P. R. Jaffé, *J. Hazard. Mater.*, 2022, **424**, 127699.

262 L. Duan, B. Wang, K. Heck, S. Guo, C. A. Clark, J. Arredondo, M. Wang, T. P. Senftle, P. Westerhoff and X. Wen, *Environ. Sci. Technol. Lett.*, 2020, **7**, 613–619.
263 L. Duan, B. Wang, K. N. Heck, C. A. Clark, J. Wei, M. Wang, J. Metz, G. Wu, A.-L. Tsai and S. Guo, *Chem. Eng. J.*, 2022, **448**, 137735.
264 T. Xu, Y. Zhu, J. Duan, Y. Xia, T. Tong, L. Zhang and D. Zhao, *Chem. Eng. J.*, 2020, **395**, 124991.
265 T. Xu, H. Ji, Y. Gu, T. Tong, Y. Xia, L. Zhang and D. Zhao, *Chem. Eng. J.*, 2020, **388**, 124230.
266 M. Qanbarzadeh, D. Wang, M. Ateia, S. P. Sahu and E. L. Cates, *ACS ES&T Engineering*, 2020, **1**, 239–248.
267 Y.-J. Lei, Y. Tian, Z. Sobhani, R. Naidu and C. Fang, *Chem. Eng. J.*, 2020, **388**, 124215.
268 J. N. Uwayezu, I. Carabante, T. Lejon, P. van Hees, P. Karlsson, P. Hollman and J. Kumpiene, *J. Environ. Manage.*, 2021, **290**, 112573.
269 F. Li, Z. Wei, K. He, L. Blaney, X. Cheng, T. Xu, W. Liu and D. Zhao, *Water Res.*, 2020, **185**, 116219.
270 W. Zhang, H. Efstathiadis, L. Li and Y. Liang, *J. Environ. Sci.*, 2020, **93**, 48–56.
271 R. J. Wood, T. Sidnell, I. Ross, J. McDonough, J. Lee and M. J. Bussemaker, *Ultrason. Sonochem.*, 2020, **68**, 105196.
272 A. J. Lewis, T. Joyce, M. Hadaya, F. Ebrahimi, I. Dragiev, N. Giardetti, J. Yang, G. Fridman, A. Rabinovich and A. A. Fridman, *Environ. Sci. Water Res. Technol.*, 2020, **6**, 1044–1057.
273 Z. Liu, Z. Chen, J. Gao, Y. Yu, Y. Men, C. Gu and J. Liu, *Environ. Sci. Technol.*, 2022, **56**, 3699–3709.
274 Y. Wang, H. Shi, C. Li and Q. Huang, *Environ. Sci. Water Res. Technol.*, 2020, **6**, 144–152.
275 D. Patch, N. O'Connor, I. Koch, T. Cresswell, C. Hughes, J. B. Davies, J. Scott, D. O'Carroll and K. Weber, *Sci. Total Environ.*, 2022, **832**, 154941.
276 D. Palma, D. Papagiannaki, M. Lai, R. Binetti, M. Sleiman, M. Minella and C. Richard, *Molecules*, 2021, **26**, 924.
277 J. Lassalle, R. Gao, R. Rodi, C. Kowald, M. Feng, V. K. Sharma, T. Hoelen, P. Bireta, E. F. Houtz and D. Staack, *Radiat. Phys. Chem.*, 2021, **189**, 109705.
278 M. S. Samuel, M. Shang and J. Niu, *Chemosphere*, 2022, **293**, 133568.
279 N. Duinslaeger and J. Radjenovic, *Water Res.*, 2022, **213**, 118148.
280 H. Olvera-Vargas, Z. Wang, J. Xu and O. Lefebvre, *Chem. Eng. J.*, 2022, **430**, 132686.
281 C. A. Martínez-Huitle and E. Brillas, *Appl. Catal. B: Environ.*, 2009, **87**, 105–145.
282 J. Niu, H. Lin, C. Gong and X. Sun, *Environ. Sci. Technol.*, 2013, **47**, 14341–14349.
283 M. Panizza, *Electrochemistry for the Environment*, 2010, pp. 25–54.
284 J. Yang, J. Wang and J. Jia, *Environ. Sci. Technol.*, 2009, **43**, 3796–3802.
285 Y. Deng and R. Zhao, *Curr. Pollut. Rep.*, 2015, **1**, 167–176.
286 K. G. Linden and M. Mohseni, Advanced Oxidation Processes: Applications in Drinking Water Treatment, *Comprehensive Water Quality and Purification*, 2014, **2**, 148–172, DOI: **10.1016/B978-0-12-382182-9.00031-1**.
287 B. P. Vellanki, B. Batchelor and A. Abdel-Wahab, *Environmental engineering science*, 2013, vol. 30, pp. 264–271.
288 D. Zhou, H. Zhang and L. Chen, *J. Chem. Technol. Biotechnol.*, 2015, **90**, 775–779.
289 Q. Yi, J. Ji, B. Shen, C. Dong, J. Liu, J. Zhang and M. Xing, *Environ. Sci. Technol.*, 2019, **53**, 9725–9733.
290 P. Attri, Y. H. Kim, D. H. Park, J. H. Park, Y. J. Hong, H. S. Uhm, K.-N. Kim, A. Fridman and E. H. Choi, *Sci. Rep.*, 2015, **5**, 1–8.
291 P. Neta, R. E. Huie and A. B. Ross, *J. Phys. Chem. Ref. Data*, 1988, **17**, 1027–1284.
292 S. Guerra-Rodríguez, E. Rodríguez, D. N. Singh and J. Rodríguez-Chueca, *Water*, 2018, **10**, 1828.
293 T. N. Das, R. E. Huie and P. Neta, *J. Phys. Chem. A*, 1999, **103**, 3581–3588.
294 S. G. Mayhew, *Eur. J. Biochem.*, 1978, **85**, 535–547.
295 H. A. Schwarz, *Free radicals generated by radiolysis of aqueous solutions*, ACS Publications, 1981.
296 P. Devi, U. Das and A. K. Dalai, *Sci. Total Environ.*, 2016, **571**, 643–657.
297 M. Hayyan, M. A. Hashim and I. M. AlNashef, *Chem. Rev.*, 2016, **116**, 3029–3085.
298 D. A. Armstrong, R. E. Huie, W. H. Koppenol, S. V. Lymar, G. Merényi, P. Neta, B. Ruscic, D. M. Stanbury, S. Steenken and P. Wardman, *Pure Appl. Chem.*, 2015, **87**, 1139–1150.
299 X. Wang and L. Zhang, *RSC Adv.*, 2018, **8**, 40632–40638.
300 R. Ossola, O. M. Jönsson, K. Moor and K. McNeill, *Chem. Rev.*, 2021, **121**, 4100–4146.
301 T. Luo, Z. Wang, Y. Wang, Z. Liu and I. P. Pozdnyakov, *Molecules*, 2019, **24**, 2307.
302 Q. Xiao, S. Yu, L. Li, T. Wang, X. Liao and Y. Ye, *J. Hazard. Mater.*, 2017, **324**, 230–240.
303 K. Hofman, N. W. Liu and G. Manolikakes, *Chem. – Eur. J.*, 2018, **24**, 11852–11863.
304 Y. Liu, X. Fan, X. Quan, Y. Fan, S. Chen and X. Zhao, *Environ. Sci. Technol.*, 2019, **53**, 5195–5201.
305 B. M. Hunter, H. B. Gray and A. M. Muller, *Chem. Rev.*, 2016, **116**, 14120–14136.
306 R. C. Forsythe and A. M. Müller, *Catal. Today*, 2022, **388**, 329–332.
307 S. Chabi, K. M. Papadantonakis, N. S. Lewis and M. S. Freund, *Energy Environ. Sci.*, 2017, **10**, 1320–1338.
308 S. Hammes-Schiffer, *Chem. Rev.*, 2010, **110**, 6937–6938.
309 D. T. Sawyer, *Oxygen radicals in biology and medicine*, 1988, pp. 11–20.
310 S. M. Mitchell, M. Ahmad, A. L. Teel and R. J. Watts, *Environ. Sci. Technol. Lett.*, 2014, **1**, 117–121.
311 W. H. Koppenol, *The Haber-Weiss cycle–70 years later*, 2001.
312 G. Ruppert, R. Bauer and G. Heisler, *J. Photochem. Photobiol. A: Chem.*, 1993, **73**, 75–78.
313 S. R. Pouran, A. A. Aziz and W. M. A. W. Daud, *J. Ind. Eng. Chem.*, 2015, **21**, 53–69.
314 S. Yang, S. Fernando, T. M. Holsen and Y. Yang, *Environ. Sci. Technol. Lett.*, 2019, **6**, 775–780.
315 D. R. Lide, *CRC handbook of chemistry and physics*, CRC Press, 2004.
316 A. J. Bard, L. R. Faulkner and H. S. White, *Electrochemical methods: fundamentals and applications*, John Wiley & Sons, 2022.
317 J. Robertson, *1.14 Free Radicals and Reactive Oxygen Species*, 2010.
318 J. L. Weeks and J. Rabani, *J. Phys. Chem.*, 1966, **70**, 2100–2106.
319 S. Yang, A. Verdaguer-Casadevall, L. Arnarson, L. Silvioli, V. Colic, R. Frydendal, J. Rossmeisl, I. Chorkendorff and I. E. Stephens, *ACS Catal.*, 2018, **8**, 4064–4081.
320 Q. Yu, R. Zhang, S. Deng, J. Huang and G. Yu, *Water Res.*, 2009, **43**, 1150–1158.
321 Y. Zhang, A. Moores, J. Liu and S. Ghoshal, *Environ. Sci. Technol.*, 2019, **53**, 8672–8681.
322 M. Trojanowicz, A. Bojanowska-Czajka, I. Bartosiewicz and K. Kulisa, *Chem. Eng. J.*, 2018, **336**, 170–199.
323 M. Umar, *Water*, 2021, **13**, 3185.
324 C. Fang, M. Megharaj and R. Naidu, *J. Adv. Oxid. Technol.*, 2017, **20**, 20170014.
325 Y. G. Song, B. Liu, L. F. Wang, M. H. Li and Y. Liu, *Photosynth. Res.*, 2006, **90**, 67–78.
326 J. Dumanović, E. Nepovimova, M. Natić, K. Kuča and V. Jaćević, *Front. Plant Sci.*, 2021, **11**, 552969.
327 T. Li, C. Wang, T. Wang and L. Zhu, *Appl. Catal. B: Environ.*, 2020, **268**, 118442.
328 H. Shi, Y. Wang, C. Li, R. Pierce, S. Gao and Q. Huang, *Environ. Sci. Technol.*, 2019, **53**, 14528–14537.
329 L. Wang, J. Lu, L. Li, Y. Wang and Q. Huang, *Water Res.*, 2020, **170**, 115254.
330 F. Zhang, Z. Sun and J. Cui, *RSC Adv.*, 2020, **10**, 33928–33936.
331 X. Liu, S. Yoon, B. Batchelor and A. Abdel-Wahab, *Chem. Eng. J.*, 2013, **215**, 868–875.
332 J. D. García-Espinoza, I. Robles, V. Gil, E. Becerril-Bravo, J. A. Barrios and L. A. Godínez, *J. Environ. Chem. Eng.*, 2019, **7**, 103228.
333 M. C. Sauer, R. A. Crowell and I. A. Shkrob, *J. Phys. Chem. A*, 2004, **108**, 5490–5502.
334 C. Fang, M. Megharaj and R. Naidu, *J. Adv. Oxid. Technol.*, 2017, **20**, 20170014.
335 M. J. Davies, *Methods*, 2016, **109**, 21–30.
336 S. Khan, X. He, J. A. Khan, H. M. Khan, D. L. Boccelli and D. D. Dionysiou, *Chem. Eng. J.*, 2017, **318**, 135–142.
337 P. Thanekar, M. Panda and P. R. Gogate, *Ultrason. Sonochem.*, 2018, **40**, 567–576.
338 K. E. O'Shea and D. D. Dionysiou, *J. Phys. Chem. Lett.*, 2012, **3**, 2112–2113.

339 T. Ochiai, Y. Iizuka, K. Nakata, T. Murakami, D. A. Tryk, A. Fujishima, Y. Koide and Y. Morito, *Diamond Relat. Mater.*, 2011, **20**, 64–67.
340 S. C. Panchangam, A. Y.-C. Lin, K. L. Shaik and C.-F. Lin, *Chemosphere*, 2009, **77**, 242–248.
341 C. Li, Y. Wang, Y. Wang, Z. Wang and Q. Huang, *J. Hazard. Mater.*, 2022, **436**, 129091.
342 J. Radjenovic, N. Duinslaeger, S. S. Avval and B. P. Chaplin, *Environ. Sci. Technol.*, 2020, **54**, 14815–14829.
343 P. Neta and R. E. Huie, *Environ. Health Perspect.*, 1985, **64**, 209–217.
344 K. G. Serrano, *Electrochemical water and wastewater treatment*, Elsevier, 2018, pp. 133–164.
345 D. Kanakaraju, B. D. Glass and M. Oelgemöller, *J. Environ. Manage.*, 2018, **219**, 189–207.
346 M. J. M. de Vidales, C. Sáez, J. F. Pérez, S. Cotillas, J. Llanos, P. Canizares and M. A. Rodrigo, *J. Appl. Electrochem.*, 2015, **45**, 799–808.
347 S. Cotillas, M. J. M. de Vidales, J. Llanos, C. Sáez, P. Canizares and M. A. Rodrigo, *J. Hazard. Mater.*, 2016, **319**, 93–101.
348 X. Shi, S. Back, T. M. Gill, S. Siahrostami and X. Zheng, *Chem*, 2021, **7**, 38–63.
349 S. Siahrostami, *Chem. Catal*, 2023, **3**, 100568.
350 K.-T. Lu, C.-C. Yang and P.-C. Lin, *J. Hazard. Mater.*, 2006, **135**, 319–327.
351 O. Špalek, J. Balej and I. Paseka, *J. Chem. Soc., Faraday Trans. 1*, 1982, **78**, 2349–2359.
352 Y. Nosaka and A. Y. Nosaka, *Chem. Rev.*, 2017, **117**, 11302–11336.
353 G. Li, X. Liu, H. Zhang, T. An, S. Zhang, A. R. Carroll and H. Zhao, *J. Catal.*, 2011, **277**, 88–94.
354 D. Zhi, Y. Lin, L. Jiang, Y. Zhou, A. Huang, J. Yang and L. Luo, *J. Environ. Manage.*, 2020, **260**, 110125.
355 C.-W. Wang and C. Liang, *Chem. Eng. J.*, 2014, **254**, 472–478.
356 F. L. Souza, C. Sáez, P. Canizares, A. J. Motheo and M. A. Rodrigo, *Appl. Catal. B: Environ.*, 2014, **144**, 121–128.
357 J. G. Speight, *Environmental organic chemistry for engineers*, Butterworth-Heinemann, 2016.
358 S. Parsons, *Advanced oxidation processes for water and wastewater treatment*, IWA Publishing, 2004.
359 H. D. Burrows, J. Santaballa and S. Steenken, *J. Photochem. Photobiol. B: Biol.*, 2002, **67**, 71–108.
360 K. Li, M. I. Stefan and J. C. Crittenden, *Environ. Sci. Technol.*, 2004, **38**, 6685–6693.
361 P. Chelme-Ayala, M. G. El-Din and D. W. Smith, *Water Res.*, 2010, **44**, 2221–2228.
362 W. Hijnen, E. Beerendonk and G. J. Medema, *Water Res.*, 2006, **40**, 3–22.
363 A. Kumar, A. Sagdeo and P. R. Sagdeo, *Photodiagnosis Photodyn. Ther.*, 2021, **34**, 102234.
364 M. Gonzalez and A. Braun, *Res. Chem. Intermed.*, 1995, **21**, 837–859.
365 T. Yamamoto, Y. Noma, S.-I. Sakai and Y. Shibata, *Environ. Sci. Technol*, 2007, **41**, 5660–5665.
366 R. R. Giri, H. Ozaki, T. Okada, S. Taniguchi and R. Takanami, *Chem. Eng. J.*, 2012, **180**, 197–203.
367 M. C. López, M. I. Fernández, C. Martínez and J. A. Santaballa, *Pure Appl. Chem.*, 2013, **85**, 1437–1449.
368 G. Liu, S. You, Y. Tan and N. Ren, *Environ. Sci. Technol.*, 2017, **51**, 2339–2346.
369 J. Prousek, *Chem. Listy*, 1996, **90**, 307–315.
370 N. F. Mott, *Mathematical Proceedings of the Cambridge Philosophical Society*, Cambridge University Press, 1938, vol. 34, pp. 568–572.
371 W. Schottky, *Naturwissenschaften*, 1938, **26**, 843.
372 N. F. Mott, *Proc. R. Soc. London, Ser. A*, 1939, **171**, 281–285.
373 W. Schottky, *Z. Phys.*, 1939, **113**, 367–414.
374 Z. Zhang and J. T. Yates Jr, *Chem. Rev.*, 2012, **112**, 5520–5551.
375 V. Hasija, P. Raizada, A. Sudhaik, K. Sharma, A. Kumar, P. Singh, S. B. Jonnalagadda and V. K. Thakur, *Appl. Mater. Today*, 2019, **15**, 494–524.
376 M. N. Chong, B. Jin, C. W. Chow and C. Saint, *Water Res.*, 2010, **44**, 2997–3027.
377 L. Jiang, X. Yuan, Y. Pan, J. Liang, G. Zeng, Z. Wu and H. Wang, *Appl. Catal. B: Environ.*, 2017, **217**, 388–406.
378 L. Clarizia, D. Russo, I. Di Somma, R. Marotta and R. Andreozzi, *Appl. Catal. B: Environ.*, 2017, **209**, 358–371.
379 J. R. Domínguez, T. González, P. Palo and E. M. Cuerda-Correa, *Ind. Eng. Chem. Res.*, 2012, **51**, 2531–2538.
380 A. Babuponnusami and K. Muthukumar, *J. Environ. Chem. Eng.*, 2014, **2**, 557–572.
381 A. Mirzaei, Z. Chen, F. Haghighat and L. Yerushalmi, *Chemosphere*, 2017, **174**, 665–688.
382 J. A. L. Perini, A. L. Tonetti, C. Vidal, C. C. Montagner and R. F. P. Nogueira, *Appl. Catal. B: Environ.*, 2018, **224**, 761–771.
383 M. Antonopoulou, C. Kosma, T. Albanis and I. Konstantinou, *Sci. Total Environ.*, 2021, **765**, 144163.
384 A. Sudhaik, P. Raizada, P. Shandilya, D.-Y. Jeong, J.-H. Lim and P. Singh, *J. Ind. Eng. Chem.*, 2018, **67**, 28–51.
385 S. Sharma, V. Dutta, P. Singh, P. Raizada, A. Rahmani-Sani, A. Hosseini-Bandegharaei and V. K. Thakur, *J. Clean. Prod.*, 2019, **228**, 755–769.
386 Y. Deng and J. D. Englehardt, *Water Res.*, 2006, **40**, 3683–3694.
387 L. Chen, J. Ma, X. Li, J. Zhang, J. Fang, Y. Guan and P. Xie, *Environ. Sci. Technol.*, 2011, **45**, 3925–3930.
388 N. Wang, T. Zheng, G. Zhang and P. Wang, *J. Environ. Chem. Eng.*, 2016, **4**, 762–787.
389 M.-H. Zhang, H. Dong, L. Zhao, D.-X. Wang and D. Meng, *Sci. Total Environ.*, 2019, **670**, 110–121.
390 J. Dong, G. Li, J. Gao, H. Zhang, S. Bi, S. Liu, C. Liao and G. Jiang, *Sci. Total Environ.*, 2022, 157695.
391 M. Xiang, M. Huang, H. Li, W. Wang, Y. Huang, Z. Lu, C. Wang, R. Si and W. Cao, *Chem. Eng. J.*, 2021, **417**, 129208.
392 L. Zhou, H. Zhang, L. Ji, Y. Shao and Y. Li, *RSC Adv.*, 2014, **4**, 24900–24908.
393 H. Che, S. Bae and W. Lee, *J. Hazard. Mater.*, 2011, **185**, 1355–1361.
394 C. Liang, C. J. Bruell, M. C. Marley and K. L. Sperry, *Chemosphere*, 2004, **55**, 1213–1223.
395 T. Ohsaka, K. Shinozaki, K. Tsuruta and K. Hirano, *Chemosphere*, 2008, **73**, 1279–1283.
396 Y. Zhong, X. Liang, Z. He, W. Tan, H. He, R. Zhu, Y. Zhong, J. Zhu, P. Yuan and Z. Jiang, *J. Nanosci. Nanotech.*, 2014, **14**, 7307–7314.
397 L. Tan, S. Lu, Z. Fang, W. Cheng and E. P. Tsang, *Appl. Catal. B: Environ.*, 2017, **200**, 200–210.
398 S. Luo, S. Yang, Y. Xue, F. Liang and C. Sun, *J. Hazard. Mater.*, 2011, **192**, 1795–1803.
399 M. Mrowetz, C. Pirola and E. Selli, *Ultrason. Sonochem.*, 2003, **10**, 247–254.
400 M. Sunder and D.-C. Hempel, *Water Res.*, 1997, **31**, 33–40.
401 M. Sansotera, F. Persico, C. Pirola, W. Navarrini, A. Di Michele and C. L. Bianchi, *Appl. Catal. B: Environ*, 2014, **148**, 29–35.
402 M. J. Bentel, Z. Liu, Y. Yu, J. Gao, Y. Men and J. Liu, *Environ. Sci. Technol. Lett.*, 2020, **7**, 351–357.
403 R. Tenorio, J. Liu, X. Xiao, A. Maizel, C. P. Higgins, C. E. Schaefer and T. J. Strathmann, *Environ. Sci. Technol.*, 2020, **54**, 6957–6967.
404 C. J. Liu, G. McKay, D. Jiang, R. Tenorio, J. T. Cath, C. Amador, C. C. Murray, J. B. Brown, H. B. Wright and C. Schaefer, *Water Res.*, 2021, **205**, 117677.
405 D. Zhang, Y. Li, X. Chen, C. Li, L. Dong and Z. Wang, *Sep. Purif. Technol.*, 2022, **287**, 120521.
406 Y.-P. Peng, H. Chen and C. Huang, *Appl. Catal. B: Environ.*, 2017, **209**, 437–446.
407 Z. U. Zango, K. S. Khoo, A. Garba, H. A. Kadir, F. Usman, M. U. Zango, W. Da Oh and J. W. Lim, *Environ. Res.*, 2023, 115326.
408 H. Tang, Q. Xiang, M. Lei, J. Yan, L. Zhu and J. Zou, *Chem. Eng. J.*, 2012, **184**, 156–162.
409 A. B. Nienhauser, M. S. Ersan, Z. Lin, F. Perreault, P. Westerhoff and S. Garcia-Segura, *J. Environ. Chem. Eng.*, 2022, **10**, 107192.
410 B. Gomez-Ruiz, S. Gómez-Lavín, N. Diban, V. Boiteux, A. Colin, X. Dauchy and A. Urtiaga, *Chem. Eng. J.*, 2017, **322**, 196–204.
411 F. Wang, K. Shih, X. Lu and C. Liu, *Environ. Sci. Technol.*, 2013, **47**, 2621–2627.
412 M. Pierpaoli, M. Szopińska, B. K. Wilk, M. Sobaszek, A. Łuczkiewicz, R. Bogdanowicz and S. Fudala-Książek, *J. Hazard. Mater.*, 2021, **403**, 123606.
413 B. Yang, J. Wang, C. Jiang, J. Li, G. Yu, S. Deng, S. Lu, P. Zhang, C. Zhu and Q. Zhuo, *Chem. Eng. J.*, 2017, **316**, 296–304.
414 X. Duan, W. Wang, Q. Wang, X. Sui, N. Li and L. Chang, *Chemosphere*, 2020, **260**, 127587.
415 A. Kugler, H. Dong, C. Li, C. Gu, C. E. Schaefer, Y. J. Choi, D. Tran, M. Spraul and C. P. Higgins, *Water Res.*, 2021, **200**, 117221.
416 A. H. da, S. Filho and G. L. de Souza, *Phys. Chem. Chem. Phys.*, 2020, **22**, 17659–17667.

417 I. Janik and G. Tripathi, *J. Chem. Phys.*, 2016, **144**, 154307.
418 H. Zipse, *Radicals in Synthesis I*, 2006, pp. 163–189.
419 C. E. Schaefer, C. Andaya, A. Urtiaga, E. R. McKenzie and C. P. Higgins, *J. Hazard. Mater.*, 2015, **295**, 170–175.
420 H. N. P. Vo, H. H. Ngo, W. Guo, T. M. H. Nguyen, J. Li, H. Liang, L. Deng, Z. Chen and T. A. H. Nguyen, *J. Water Process Eng.*, 2020, **36**, 101393.
421 R. De Marco, G. Clarke and B. Pejcic, *Electroanalysis*, 2007, **19**, 1987–2001.
422 D. R. Taves, *Nature*, 1968, **217**, 1050–1051.
423 J. L. Barber, U. Berger, C. Chaemfa, S. Huber, A. Jahnke, C. Temme and K. C. Jones, *J. Environ. Monit.*, 2007, **9**, 530–541.
424 K. L. Rodriguez, J.-H. Hwang, A. R. Esfahani, A. A. Sadmani and W. H. Lee, *Micromachines*, 2020, **11**, 667.
425 A. U. Rehman, M. Crimi and S. Andreescu, *Trends Environ. Anal. Chem.*, 2023, e00198.
426 Z. Wang, J. C. DeWitt, C. P. Higgins and I. T. Cousins, *Environ. Sci. Technol.*, 2017, 2508–2518.
427 Y. Liu, L. A. D'Agostino, G. Qu, G. Jiang and J. W. Martin, *TrAC, Trends Anal. Chem.*, 2019, **121**, 115420.
428 I. Kourtchev, S. Hellebust, E. Heffernan, J. Wenger, S. Towers, E. Diapouli and K. Eleftheriadis, *Sci. Total Environ.*, 2022, **835**, 155496.
429 D. Camdzic, R. A. Dickman, A. S. Joyce, J. S. Wallace, P. L. Ferguson and D. S. Aga, *Anal. Chem.*, 2023, **95**, 5484–5488.
430 J. N. Dodds, Z. R. Hopkins, D. R. Knappe and E. S. Baker, *Anal. Chem.*, 2020, **92**, 4427–4435.
431 R. C. Forsythe, C. P. Cox, M. K. Wilsey and A. M. Muller, *Chem. Rev.*, 2021, **121**, 7568–7637.
432 M. K. Wilsey, C. P. Cox, R. C. Forsythe, L. R. McCarney and A. M. Müller, *Catal. Sci. Technol.*, 2021, **11**, 416–424.
433 P. C. Vesborg and T. F. Jaramillo, *RSC Adv.*, 2012, **2**, 7933–7947.
434 Z. W. Seh, J. Kibsgaard, C. F. Dickens, I. Chorkendorff, J. K. Nørskov and T. F. Jaramillo, *Science*, 2017, **355**, eaad4998.
435 C. C. McCrory, S. Jung, J. C. Peters and T. F. Jaramillo, *J. Am. Chem. Soc.*, 2013, **135**, 16977–16987.
436 S. Nitopi, E. Bertheussen, S. B. Scott, X. Liu, A. K. Engstfeld, S. Horch, B. Seger, I. E. Stephens, K. Chan and C. Hahn, *Chem. Rev.*, 2019, **119**, 7610–7672.
437 R. Schlögl, *Angew. Chem., Int. Ed.*, 2015, **54**, 3465–3520.
438 H. Topsøe, *J. Catal.*, 2003, **216**, 155–164.
439 B. M. Weckhuysen, *Phys. Chem. Chem. Phys.*, 2003, **5**, 4351–4360.
440 Y.-W. Choi, H. Mistry and B. R. Cuenya, *Curr. Opin. Electrochem.*, 2017, **1**, 95–103.
441 B. M. Hunter, N. B. Thompson, A. M. Müller, G. R. Rossman, M. G. Hill, J. R. Winkler and H. B. Gray, *Joule*, 2018, **2**, 747–763.
442 N. Omidvar, H. S. Pillai, S.-H. Wang, T. Mou, S. Wang, A. Athawale, L. E. Achenie and H. Xin, *J. Phys. Chem. Lett.*, 2021, **12**, 11476–11487.
443 S. Gusarov, S. R. Stoyanov and S. Siahrostami, *J. Phys. Chem. C*, 2020, **124**, 10079–10084.
444 Y. Yang, C. R. Peltier, R. Zeng, R. Schimmenti, Q. Li, X. Huang, Z. Yan, G. Potsi, R. Selhorst and X. Lu, *Chem. Rev.*, 2022, **122**, 6117–6321.
445 S. Liu, L. D'Amario, S. Jiang and H. Dau, *Curr. Opin. Electrochem.*, 2022, **35**, 101042.
446 L. Lukashuk, N. Yigit, R. Rameshan, E. Kolar, D. Teschner, M. Hävecker, A. Knop-Gericke, R. Schlögl, K. Föttinger and G. N. Rupprechter, *ACS Catal.*, 2018, **8**, 8630–8641.
447 B. S. Yeo and A. T. Bell, *J. Phys. Chem. C*, 2012, **116**, 8394–8400.
448 D. Friebel, M. W. Louie, M. Bajdich, K. E. Sanwald, Y. Cai, A. M. Wise, M.-J. Cheng, D. Sokaras, T.-C. Weng and R. Alonso-Mori, *J. Am. Chem. Soc.*, 2015, **137**, 1305–1313.
449 H.-J. Lewerenz, M. F. Lichterman, M. H. Richter, E. J. Crumlin, S. Hu, S. Axnanda, M. Favaro, W. Drisdell, Z. Hussain and B. S. Brunschwig, *Electrochimica Acta*, 2016, **211**, 711–719.
450 S. J. Blair, M. Doucet, V. A. Niemann, K. H. Stone, M. E. Kreider, J. F. Browning, C. E. Halbert, H. Wang, P. Benedek, E. J. McShane, A. C. Nielander, A. Gallo and T. F. Jaramillo, *Energy Environ. Sci.*, 2023, **16**, 3391–3406.
451 F. Dionigi, Z. Zeng, I. Sinev, T. Merzdorf, S. Deshpande, M. B. Lopez, S. Kunze, I. Zegkinoglou, H. Sarodnik and D. Fan, *Nat. Commun.*, 2020, **11**, 2522.
452 C. D. Taylor, S. A. Wasileski, J.-S. Filhol and M. Neurock, *Phys. Rev. B*, 2006, **73**, 165402.
453 A. Bruix, J. T. Margraf, M. Andersen and K. Reuter, *Nat. Catal.*, 2019, **2**, 659–670.
454 T. Van Mourik, M. Bühl and M.-P. Gaigeot, *Phil. Trans. R. Soc. A*, 2014, **372**, 20120488.
455 S. Siahrostami, A. Verdaguer-Casadevall, M. Karamad, D. Deiana, P. Malacrida, B. Wickman, M. Escudero-Escribano, E. A. Paoli, R. Frydendal and T. W. Hansen, *Nat. Mater.*, 2013, **12**, 1137–1143.
456 A. D. White and G. A. Voth, *J. Chem. Theory Comput.*, 2014, **10**, 3023–3030.
457 J. T. Margraf, *Angew. Chem.*, 2023, e202219170.
458 Y. Chen, Y. Huang, T. Cheng and W. A. Goddard III, *J. Am. Chem. Soc.*, 2019, **141**, 11651–11657.
459 M. Neurock, M. Janik and A. Wieckowski, *Faraday Discuss.*, 2009, **140**, 363–378.
460 E. I. Solomon, R. A. Scott and R. B. King, *Computational inorganic and bioinorganic chemistry*, John Wiley & Sons, 2013.
461 D. Rappoport, N. R. Crawford, F. Furche and K. Burke, *Encyclopedia of Inorganic Chemistry*, 2006.
462 K. Kim, P. Baldaguez Medina, J. Elbert, E. Kayiwa, R. D. Cusick, Y. Men and X. Su, *Adv. Funct. Mater.*, 2020, **30**, 2004635.
463 M. J. Bentel, Y. Yu, L. Xu, H. Kwon, Z. Li, B. M. Wong, Y. Men and J. Liu, *Environ. Sci. Technol.*, 2020, **54**, 2489–2499.
464 Y. Zhang, M. Dai and Z. Yuan, *Anal. Methods*, 2018, **10**, 4625–4638.
465 R. Guo, B. Xi, C. Guo, N. Lv and J. Xu, *Environ. Funct. Mater.*, 2022, 67–91.
466 J. Wang and S. Wang, *Chem. Eng. J.*, 2020, **401**, 126158.
467 S. Stoll and D. Goldfarb, *EPR spectroscopy: fundamentals and methods*, John Wiley & Sons, 2018.
468 M. M. Roessler and E. Salvadori, *Chem. Soc. Rev.*, 2018, **47**, 2534–2553.
469 S. Stoll and R. D. Britt, *Phys. Chem. Chem. Phys.*, 2009, **11**, 6614–6625.
470 H. E. Williams, V. C. Loades, M. Claybourn and D. M. Murphy, *Anal. Chem.*, 2006, **78**, 604–608.
471 A. Gomes, E. Fernandes and J. L. Lima, *J. Biochem. Biophys. Methods*, 2005, **65**, 45–80.
472 J. Wang, Y. Guo, B. Liu, X. Jin, L. Liu, R. Xu, Y. Kong and B. Wang, *Ultrason. Sonochem.*, 2011, **18**, 177–183.

